
*Towards a better interpretation of
bone morphology: The effect of
obesity on bone*

THOMAS ATTERTON

A thesis submitted in partial fulfilment of the requirements of Liverpool John Moores
University for the degree of Master of Philosophy

September 2016

Contents

Abstract.....	3
Introduction	4
Bone: an active tissue	4
Factors affecting bone	7
Assessing body mass in past populations	10
Impact of obesity on Bone Health	14
Impact of obesity on living human bone	18
Animal models	20
Aim's and objectives	22
Materials and Methods.....	23
Animals and experimental design.....	23
Sample preparation and transportation.....	25
Micro-CT.....	25
Dissection.....	26
Measurement acquisition	26
Data analyses	31
Results.....	36
Linear measurement comparisons	36
Geometric morphometric shape analyses.....	42
Cross-sectional shape analyses.....	46
Body mass Analysis	52
Discussion	54
Conclusion.....	59
References	62

Abstract

The effects of obesity on bone are poorly understood in biological anthropology. By using an experimental approach, we hope to achieve several aims and objectives designed to further our understanding of how obesity affects bone health. The aims also look at trying to understand the implications of the results for understanding past human populations and modern day issues surrounding obesity. To accomplish this, a project has been developed and is outlined below.

Bones from lean (control), obese and calorie restricted rats (n=9 rats/group) that were raised in metabolic cages and sacrificed at 17 weeks of age, were studied. The samples were provided by the Nutrition and Obesity Research Group of the University of the Basque Country. The carcasses were micro-CT scanned for linear measurements (LM), geometric morphometric shape analysis (GMSA) and cross sectional shape analysis (CSSA).

LM, GMSA and CSSA were performed on a set of 18 landmarks representing the overall shape of the right femur, using the MorphoJ package and Avizo 9.0 software. Cross-sections were obtained at the midshaft and the most lateral point of the third trochanter. The following measurements were collected: maximum length, epiphysis diameter, epiphysis circumference, epicondyle width and epiphysis/epicondyle width ratio. Obese rats had significantly longer but narrower femora.

The LM, GMSA and CSSA significantly differentiated between control, obese and calorie restricted. Obese individuals had longer femora with a relatively higher positioned third trochanter but were more gracile and weaker in their diaphyseal strength and rigidity compared to the control sample. These findings confirm that obesity has a significant effect on bone shape and strength but the results from the calorie restricted group demonstrates that these may be reversible. Further research into potential underlying mechanisms, including interactions between bone and lipid cells is required.

Introduction

This study provides a novel approach to studying the effect of obesity on bone morphology – a topic poorly investigated in the field of study of human skeletons. By using an experimental approach utilising rats as models, a project has been developed within the field of anthropology that has current relevance and societal impact. The aims of the research project were twofold: 1. To provide crucial information of the influence of diet and obesity on bone morphology of past human populations; 2. To address current societal challenges, including obesity, on bone health. However, before we can interpret effects of diet and obesity on bone, we must have a better understanding of bone composition.

Bone: an active tissue

Bone can simply be defined as the biological material that protects the internal organs and supports the human body. It consists of living cells, osteoblasts, osteoclasts and osteocytes which are discussed below, embedded in a mineralised matrix of collagen. However, bone quality is not so easily defined. This is discussed by Bouxsein (2003) as there is an increasing interest in how bone quality effects strength of bone, especially in those with osteoporosis to develop treatments. Bone quality has been associated with several factors due to inconsistent use of the term such as trabecular architecture, bone turnover, organic/inorganic composition of bone, type and amount of collagen crosslinks, matrix mineralisation, microdamage accumulation and cell viability (Bouxsein, 2003). As such, bone quality is associated with any measurement of bone that can influence the effectiveness of its purpose, i.e. its ability to protect and act as a support structure.

Before any interpretations can be made on bone quality it is important to understand the differences between the three main bone cell types to fully appreciate and interpret the results with regards to skeletal biomechanics and its biological impact. Osteoblasts are responsible for bone growth which is a very complex process. The main function of an osteoblast is to produce and secrete proteins that create a bone matrix (Robey and Boskey, 1995). Following the matrix creation, the osteoblast then mineralises the matrix. The three main proteins secreted by osteoblasts are type I collagen, osteocalcin and osteonectin (Manolagas, 2000). Type I collagen is used to create the initial bone matrix

and accounts for the majority of the proteins used to form bone. The type I collagen undergoes a process that removes its propeptides, resulting in the collagen becoming mature three-chained type I collagen molecules. These are able to assemble themselves as collagen fibrils, unique to bone (Manolagas, 2000). Osteocalcin and osteonectin make up approximately 40-50% of the proteins found in bone and between them have very different roles (Manolagas, 2000). Osteocalcin is thought to act as a limiter to bone formation without compromising bone mineralisation (Ducy, et al., 1996). This may sound detrimental, however, without the osteocalcin restricting bone growth, bone can become cancellous and osteoclast performance can be impacted (Ducy, et al., 1996). Osteonectin plays a role in the development and survival of osteoblasts, which has major effects on bone remodelling (Ducy, et al., 1996), with mice deficient in osteonectin developing profound osteopenia (Ducy, et al., 1996).

As previously mentioned, osteoblasts do not solely create bone matrix using type I collagen, they also mineralise bone by depositing hydroxyapatite onto newly created bone matrix (Boskey, 1998; Boskey, 1996). The hydroxyapatite formation is thought to be promoted by osteoblasts regulating local concentrations of calcium and phosphate (Manolagas, 2000). Osteoblasts also have a high concentration of alkaline phosphatase in their plasma membrane, which has been reported to play a role in bone mineralisation (Manolagas, 2000). Alkaline phosphatase deficiency, which is due to genetic defects, leads to hypophosphatasia which is a condition characterised by defective bone mineralisation (Whyte, 1994). Another important factor of bone mineralisation is its effect on bone density and bone volume. Mineralisation of bone matrix increases bone density as it displaces the water from the matrix but has no effect on the volume of bone (Manolagas, 2000).

Osteocytes act as a 'nervous system' for bone and are buried in lacunae of mineralised matrix. This terminology is used based on morphological similarities displayed by both osteocytes and the dendritic network of the nervous system (Palumbo, et al., 1990; Nijweide, et al., 1996). Osteocytes are the most abundant bone cell type and are regularly spaced through the mineralised bone matrix in order to communicate with each other and the surface lining cells of bone (Manolagas, 2000). In order to communicate with all the other cell types in the bone, osteocytes have multiple extensions of their plasma

membranes that run along canaliculi, enabling them to reach the lining cells and the osteoblasts (Manolagas, 2000). This communication between the cells makes osteocytes the perfect mechanosensory cells for bone and allows the body to identify and target any changes in the bone. These changes may require bone augmentation and reinforcement or bone reduction. They would also be able to detect any micro-damage and fatigue in the bone and repair the damage before the bone fails (Aarden, et al., 1994). Osteocytes are also able to determine changes to interstitial fluid which flows through canaliculi and also hormone levels of estrogen and glucocorticoids (Weinstein, et al., 1998; Tomkinson, et al., 1998; Tomkinson, et al., 1997).

Osteoclasts are the bone resorption cells and play a major role in bone remodelling and the precursor to bone augmentation. Osteoclasts are also the largest of the three main cell types and are multinucleated cells with abundant mitochondria, free ribosomes and numerous lysosomes (Manolagas, 2000). In addition to these important cell morphologies, the osteoclasts have two further distinct morphological features. The first is the ruffled border which is a complex system on projections of the membrane, which mediates calcified bone matrix resorption (Roodman, 1996; Boskey, 1998). The second feature is a specialised area called the clear zone where the cytoplasm has a uniform appearance and contains actin-like filament bundles (Manolagas, 2000). This clear zone acts as a seal between the cell and the resorption area, allowing a microenvironment to be formed that is suitable for the resorption of bone. De-mineralisation occurs when the mineralised matrix is exposed to the acidic environment of the resorption site beneath the ruffled border. This is created by the ATP-driven proton pump located in the ruffled border (Manolagas, 2000). After de-mineralisation, the matrix is degraded through matrix metalloproteinases, followed by osteoclast secretion of cathepsins K B and L into the area of bone resorption (Bossard, et al., 1996). The components of the bone matrix are then transcytosed to the opposite membrane to the bone to be released (Nesbitt and Horton, 1997; Salo, et al., 1997). Osteoclasts also have high amounts of phosphohydrolase enzymes. Tartrate-resistant acid phosphatase (TRAPase) is a marker enzyme used to identify osteoclasts in bone specimens (Udagawa, et al., 1990). It has been shown in studies that mice deficient in TRAPase, have defective mineralisation of cartilage in developing bones (Hayman, et al., 1996)

Lining cells, also found within bones, are generated from osteoblasts (much like osteocytes) and display a flat and elongated morphology. They are found covering un-mineralised collagen matrix above normal bone that is not undergoing remodeling (Parfitt, 1994). The main function of the lining cells is to prevent the attachment of osteoclasts and prevent unwanted bone remodeling. It is thought that osteocytes send a signal to areas of lining cells to secrete collagenase which removes the lining cells before remodeling (Roodman, et al., 1996) therefore allowing remodeling to occur in a controlled way.

By understanding all the above cell types and their roles we can interpret the limited responses of bone (resorption and creation) in different ways. For example, if bone loss is occurring without the creation of bone, we can determine bone is simply being lost. However, if we see bone resorption and bone matrix creation in the same area, we know that bone is being re-modelled to facilitate new stimuli in an area, and is not necessarily negative. These factors will have a role to play in the interpretation of the impact of obesity on bone health.

Factors affecting bone

All the above cell types are important for maintaining homeostasis in the bone with emphasis being placed on the osteocytes. As discussed by Prideaux et al (2016), the osteocytes control the pathways between all bone cell types using the extensive network of canaliculi throughout the bone matrix. Therefore, the osteocytes control both bone formation and resorption by osteoblasts and osteoclasts, ultimately controlling the reaction of bone to external and internal stimuli. Prideaux et al (2016) also summarised which factors controlled by osteoclasts affect which bone cell along with the outcome of the factor response (Table 1).

Table 1: Osteocyte-derived factors and their roles in bone remodelling Based on Table 1 found in Prideaux et al (2016)

[The Table originally presented here cannot be made freely available via LMU E-Theses Collection because of copyright. The table can be sourced at Prideaux et al (2016), table 1, page 27]

A review article by De Fusco, et al (2017) looks at the relationship between adipose tissue and bone homeostasis to try and understand how obesity and osteoporosis are linked. This connection is made by looking at osteopontin (OPN) which is a protein associated with bone metabolism and remodelling, but also in the pathogenesis of obesity and osteoporosis. The review by De Fusco, et al, (2017) found that there is evidence supporting a cytokine and hormonal crosstalk between bone cells, liver cells and adipose tissue caused by OPN. This crosstalk regulates bone remodelling, energy metabolism and glucose homeostasis which when changed may lead to obesity and other disorders such as type II diabetes (De Fusto, et al, 2017). This leads to further questions such as does altering adipose tissue quantities (obesity) affect bone homeostasis? This study hopes to further this understanding and help answer this question by analysing the bone quality of an experimental sample.

Another factor which can affect bone homeostasis and its structure/microstructure is mechanical stimuli and exercise. As discussed by Forwood and Burr (1993) exercise during development can add significant amounts of cortical and trabecular bone and these trends can be maintained throughout adulthood. However, Forwood and Burr (1993) also mention that too much exercise can negatively affect bone growth, as the stimuli can suppress normal growth and modelling activities of bone.

The opposite of exercise is disuse, which has been studied through bed rest and space exploration studies. Carmeliet and Bouillon (2001) investigated both types of studies and found that in general, when bone is unloaded, bone formation is decreased and bone resorption is unaltered or increased. Carmeliet and Bouillon (2001) also found that the changes are reversible, but recovery time is far greater than the period of unloading.

Sex and age are also factors which can have dramatic effects on bone and its changes throughout a lifetime. The general rule is that as bone ages, it becomes weaker, with less bone being created and more being resorbed. However, these changes with age are not uniform between sexes. This is discussed by Khosla, et al (2006) who performed a population based cross-sectional study, on the effects of age and sex on bone microstructure at the wrist. The first findings of Khosla, et al (2016) are that young men (20-29 years) have a significantly greater trabecular volume/tissue volume and trabecular thickness than young women. However, the values for trabecular number and trabecular

separation were similar (Khosla, et al, 2016). With age, women appear to have greater decreases in trabecular numbers and increases in trabecular space in comparison with men (Khosla, et al, 2016). Men however lose a significant amount of trabecular thickness in comparison to women with age (Khosla, et al, 2016).

Assessing body mass in past populations

Of particular interest in the field of anthropology is the necessity to understand obesity in past human populations. Paleoanthropologists and bioarchaeologists have struggled in the past to distinguish between markers of high body mass and markers of activity in the fossil and archaeological record. Using cross-sectional analysis to study bone strength, several authors were able to differentiate between habitual activities of individuals with good results, showing that this type of analysis can be used to differentiate between differing lifestyles (Ruff, 1987; Sarringhaus, et al., 2005; Shaw and Stock, 2009; Stock, 2002; Stock and Pfeiffer, 2004; Stock and Shaw, 2007). These methods are not frequently applied in the field of physiology but are very suitable to understand morphological changes in cross-sections in our samples. For example, the study by Ruff (1987) utilised cross-sectional analysis to identify sexual division of labour in a late pre-historic archaeological sample from Pecos Pueblo, New Mexico and also a modern U.S. white sample. Ruff (1987) summarises that the largest area of variation for identifying sexual division of labour can be seen in the cross-sections closest to the knee which may be related to subsistence strategy. Also, Ruff (1987) introduced the idea that sexual dimorphism in long bones may be affected by habitual activities during life. These methods do not only work in humans but also in other animals. Sarringhaus et al. (2005) used cross-sectional analysis of the left and right humeri to identify handedness in chimpanzees. This study identified an asymmetry in the upper limbs of chimpanzees, which was linked to handedness. In humans, handedness was also demonstrated as Shaw and Stock (2009) compared modern human athletes to identify areas of correspondence in upper limb diaphyseal strength and shape. In order to achieve this, Shaw and Stock (2009) studied a group of swimmers, cricketers and a control group and found that both the swimmers and cricketers consistently displayed changes in the upper limb. The swimmers showed symmetrical strengthening across both left and right upper limbs, whereas the cricketers showed strengthening in dominant arms, leading to asymmetric

results. Stock and Pfeiffer (2004) used long bone diaphysis analysis to investigate sexual dimorphism and sexual division of labour between two different terrain environments of South Africa in the Stone Age. The first environment was a forest biome where Stock and Pfeiffer (2004) reported that there was a greater disparity in manual labour in the forest biome. The second biome studied was a fynbos biome. This group was found to have a greater disparity in terrestrial mobility, suggesting that the males travelled much further distances than the females. More recently, Ruff (2008) has used the cross-sectional analysis technique to help identify bipedalism in ancient human remains by comparing the bone strength of femora between modern humans and chimpanzees and found that the technique was capable of distinguishing between bipeds and quadrupeds.

Throughout the literature, several different methods are used to study cross-sectional morphology. The paper by Stock (2002) was a crucial step forward in cross-sectional analysis methodology. It was the first in which three methods were directly compared. The three methods tested by Stock (2002) were; direct sectioning (DS), eccentric elliptical method (EEM) and the latex cast method (LCM). Direct sectioning is the process of physically creating a cross-section by sawing a bone at the required location. This method provides the most accurate results but destroys samples. Therefore, this is only used in tightly controlled environments and scenarios where the bones have broken naturally, allowing for a cross-section to be taken directly. EEM uses bi-planar radiographs to measure the thickness of bone on all four sides of the diaphysis and combines these with external caliper measurements. Using these measurements, two ellipses are calculated. One is calculated using the exterior measurements and a second is calculated using internal measurements. The second ellipse is then placed eccentrically inside the first ellipse, giving an estimated cross-section of the sample. LCM uses the same principal of the EEM but uses a latex cast of the exterior of the sample to more accurately represent the circumference. The internal ellipse calculations are then placed inside the actual area of the sample resulting in only the internal ellipse to be estimated from the radiographs. If sample preservation is not required then DS is always the most accurate methodology of choice, however in the majority of cases, this is not an acceptable technique. Recent applications of CT scanning of archaeological samples have allowed for the capture of the cross-sectional measurements without direct sectioning. Nevertheless, this method is

expensive and CT scanners are not always available. Furthermore, in living humans the radiation exposure associated with CT scanning poses a risk to the individual. LCM gives results within a 5% variance of DS and EEM only gives accurate results for the areas of bone studied and not for second moments of area, used for biomechanical analysis (Stock, 2002). Therefore, for this study, the principles of LCM were used to determine cross-sectional strength analysis of the bones. However, instead of using a cast of the bones, the CT Scans were used, giving a much higher resolution image. Stock and Shaw (2007) also designed a study to test and improve the experimental procedure of cross-sectional analysis by understanding the impact of correct standardisation for body mass and bone length in biomechanical analyses. Estimating activity levels from skeletal elements has therefore been confounded by the ability to estimate body mass accurately from the skeleton. The femoral head is most frequently used to estimate body mass, but has been demonstrated to reflect body mass at the age of femoral head fusion (around 18 years) (Ruff, 1991). This may not accurately reflect the actual weight of the individual as an adult. Another method that has been validated for use is the stature/bi-iliac breadth (STBIB). Auerbach and Ruff (2004) discuss both of the above techniques and compare them to determine which is the most accurate for future application. The findings from Auerbach and Ruff (2004) suggest that the two techniques are comparable and both are equally accurate. Since the body mass of the rodents is known in this study, further signals and estimations of body mass may be identified.

Most clinical studies investigating physical activity and bone health have only looked at bone strength but not morphology (Burr, 1997; Felsenberg and Boonen, 2005). In adults, activity contributes to skeletal maintenance, enhanced bone density (Madsen, et al., 1998) and has been shown to prevent and delay the onset of post-menopausal osteoporosis (Kanders, et al., 1988). However, a recent study by Rabey et al. (2015) suggested that although activity stimulates bone and muscle growth, it does not affect muscle attachment site (enthesis) size. Further, a study by Zumwalt (2006) reported that activity levels have no direct causal relationship with entheses size and that there is also no link between actual muscle size and enthesal morphology. Both of these studies used highly controlled experimental set ups, unlike the majority of previous anthropological studies such as those by Weiss (2007) and Lee and Piazza (2009), where musculoskeletal

markers are used as direct indicators of past activities and living habits. This may suggest muscle attachment size is affected by other factors. Villotte et al. (2010) have suggested diet, gender and age may all have a significant effect on muscle attachment site size. The history of using enthesal changes to measure activity has undergone many variations since 1983, as reflected in name changes also (Jurmain, et al. 2012); “activity induced pathology” (Merbs, 1983), “evidence for occupation” (Kelley and Angel, 1987), “skeletal markers of occupational stress” (Kennedy, 1989), “activity induced stress markers” (Hawkey and Street, 1992) and the more recent change to “enthesal changes” (Jurmain and Villotte, 2010). The field of physical anthropology has historically been critiqued for over-simplified methodologies and also over-interpreting results when it comes to developing methods of measuring complex factors, such as bone shape (Villotte and Knüsel, 2013). More recently however, the emphasis has been to standardise the field and to improve the findings of results through experimental means and environmental factor isolation (Rabey, et al., 2015; Zumwalt, 2006). It is necessary therefore to identify skeletal characteristics that will allow researchers to distinguish more accurately between the effects of activity and those of body mass on bone morphology and strength. It is for this reason that this project will consider muscle attachment sites as part of bone morphology by using geometric morphometric analysis of the third trochanter on the femur.

Evidence of obesity already exists from the upper Palaeolithic time period (45,000 – 10,000 BP) through the Venus idols (Józsa, 2011). Józsa (2011) examined 97 female idols found across most Eurasia of which 51 represented overweight or obese females. One theory behind the Venus idol’s, the first of which is that they represent female fertility, however only 7 of the idols studied by Józsa (2011) appear to be pregnant, which makes this theory seem more unlikely. It is also impossible to know whether these idols were accurate representations of real individuals, or ideals that were sought after. This could only be proven by examining the remains of the population and currently there is no accurate/reliable method to determine full physiology from bone. However, this study aims to address obesity and its impact on bone to further shine a light on past populations and the true physiology they displayed.

Impact of obesity on Bone Health

Obesity is defined as an excess in adipose tissue as discussed by Guillaume (1999).

However, obesity is difficult to measure and as such several methods for use in both lab and field have been developed, each with their own strengths and weaknesses. The lab based methods are as follows; densitometry, hydrometry, dual energy X-ray absorptiometry (DXA) and imaging techniques.

Densitometry uses the assumption that body fat consists as two distinct areas within the body, fat mass (FM) and fat free mass (FFM) each with their own distinct density, 0.9Kg/l and 1.1Kg/l respectively (Deurenberg and Yap, 1999; Jebb and Elia, 1993). This assumption, and the known density of an individual, usually calculated through water displacement, leads to the calculation of FM and FFM ratio, with a lower ratio meaning higher levels of fat. This method has many drawbacks however, the main one of which is the unknown value of air trapped within the lungs and gut that can alter the density measurements, meaning corrections must be made.

Hydrometry uses suitable tracers such as deuterium oxide, tritium oxide or ¹⁸O-labelled water, to determine the total body water (TBW) (Deurenberg and Yap, 1999; Jebb and Elia, 1993). This technique also calls on assumptions made in densitometry around the groups of FM and FFM, as only FFM contains water. After the selected tracer has had adequate equilibrium time, the tracer concentration in blood, saliva urine or expired water is determined in order to calculate TBW. In addition to this, it is assumed that hydration of FFM is kept at 73% based on carcass analyses (Deurenberg and Yap, 1999). Using the FFM hydration assumption of 73%, total FFM can be calculated, which when used with weight allows the calculation of FM and body fat percentage. The main drawback of this technique is the assumption of FFM hydration level being 73%, as if this is wrong it can significantly impact results. However, if this assumption is accurate, the results have an error of less than 1% (Duerenberg and Yap, 1999).

DXA was developed to study osteoporosis and uses two different energy levels of x-ray, based on the different attenuation coefficients of soft tissue and minerals on the one hand and between fat and lean tissue on the other (Duerenberg and Yap, 1999; Pietrobelli, et al, 1996). This method has a low technical error for body fat percentage,

between 1 and 3%, however there is dispute over the technique as different softwares and machines can give different results (Duerenberg and Yap, 1999). Also, tissue depth can affect the total attenuation of the body, meaning that this method has different accuracies between obese and lean individuals (Duerenberg and Yap, 1999).

The imaging techniques mentioned above consist of magnetic resonance imaging (MRI) and computed tomography (CT). MRI and CT are very similar in the fact that they allow three-dimensional information of body composition to be collected. The main difference between the two techniques is that CT uses several x-ray images of the same area from different angles to compute three-dimensional data, whereas MRI uses the magnetic resonance of water content in the body to do the same task. However, due to the methodological differences in how this data is collected, MRI is more suited to soft tissue and CT more suited to hard tissue. Even though these techniques are extremely accurate and the method of choice for most researchers, both techniques suffer from high costs and time constraint issues, as the equipment is usually located in hospitals and used for medical procedures.

There are also several field based techniques that can be used to identify obesity and body fat percentages. These methods are; skinfold thickness measurements, bio-electrical impedance and body mass index (BMI).

Skinfold thickness measurements assume that the relationship between subcutaneous fat and total body fat is constant throughout the body (Duerenberg and Yap, 1999). Using several skinfold locations such as the upper arm, under the scapula and above the iliac crest a trained observer can calculate body fat percentage using equations such as those developed by Durnin and Womersley (1974). The error in body fat percentage in direct comparison with densitometry is 3-5% (Duerenberg and Yap, 1999), but this may be higher in obese individuals as the skinfolds are harder to measure, even for trained individuals.

Bio-electrical impedance assumes that only body water and its electrolytes can conduct electricity throughout the human body, meaning that body water and body impedance are inversely related. Therefore, using a small alternating current resistivity can be measured, and assuming that the body is cylindrical in shape, a prediction model

including height²/impedance can be used as a predictor for obesity (Duerenberg and Yap, 1999). However, this method, although easy to apply has several sources of error. The first of these is that the distribution of body water is not equal, with each area of body water having different measures of resistivity. This is further impacted by body shape and build as individuals with longer extremities tend to have an over estimation in body fat percentage.

BMI is a corrected measure of weight for height, and is used as a crude index for assessing obesity in individuals with ease. The technique relies upon a high correlation between weight/height index and body fat as well as a low correlation with body height (Duerenberg and Yap, 1999). The main drawback of BMI is the major assumption that body fat distribution is equal amongst all people and as such over simplifies the measurement. However, the speed and ease of the measurement means that it can be quickly used to roughly assess the general health of an individual by health professionals and researchers.

Dietary changes to the body due to over-nutrition have negative impacts and can lead to several health conditions such as obesity (Lloyd and Wolff, 1980) and immunodeficiency (Chandra, 1981). The prevalence of obesity is increasing globally and is a major problem. Obesity is classified using the body mass index (BMI) scale which uses a person's height and weight to create a ratio value ($BMI = \text{Weight [Kg]} / \text{Height[m]}^2$). A value between 18 and 25 is considered normal, 25-30 is overweight and >30 is obese (Bose, et al., 2007). Obesity is well reported to be extremely detrimental to a person's health leading to several conditions such as cardiovascular disease, type II diabetes, high blood pressure, high cholesterol, asthma and osteoarthritis (Mokdad, et al., 2001; Must, et al., 1999).

Cardiovascular disease is the general grouping term for conditions which include heart disease, stroke and heart failure (Eckel, et al., 2006). The link between cardiovascular disease and obesity is complicated by lifestyle factors which can themselves influence the disease such as smoking, hypertension, high cholesterol, and dysfunctions in glucose metabolism (Van Gaal, et al., 2006). However, obesity is one of the main causes of cardiovascular disease, and as such the American Heart Association (AHA) has reclassified obesity as a major risk factor for cardiovascular disease (Eckel, et al., 2006; Van Gaal, et al., 2006). Obesity is also known to be a risk factor for heart failure, leading to a higher

mortality rate in obese individuals (Kenchiah, et al., 2002). Diabetes and obesity have historically gone hand in hand and the two are strongly associated (Steppan, et al., 2001). Type II Diabetes is caused by a resistance to insulin but the exact mechanism that causes resistance due to obesity is unclear. However, a hormone called resistin has been found that potentially links obesity to diabetes (Steppan, et al., 2001).

High blood pressure is defined as mean systolic blood pressure ≥ 140 mmHg and or mean diastolic blood pressure ≥ 90 mmHG. Obesity has strong links to high blood pressure with 38.4% of obese men and 32.2% of obese women having high blood pressure compared to 18.2% and 16.5% for men and women respectively with healthy weights (Bose, et al., 2007). High cholesterol has been shown to be more prevalent in women than men (Brown, et al., 2000), but is still a problem for both genders in relation to obesity (Denke, et al., 1994). With regards to cholesterol levels, it appears that levels are higher in persons with large abdominal fat deposits (Bose, et al., 2007).

It has also been recently suggested that there is a link between obesity and asthma, with obesity being a predisposing factor (Boulet, 2013). However, the exact cause of asthma due to obesity is still under discussion. Osteoarthritis is also a high risk health problem for the obese individual (Bose, et al., 2007; Denke, et al., 1994; Boulet, 2013; Hart and Spector, 1993) and it is estimated that for every kilogram gained, osteoarthritis development risk increases by 9-13% for both genders (Cicuttini, et al., 1996).

Due to the severity of the health issues associated with obesity its worldwide prevalence (Ng, et al., 2013), obesity has recently become one of the most important issues from both a financial and a healthcare perspective (Mokdad, et al., 1999). Specifically in the United states where one third of adults and 17% of sub-adults are obese (Ogden, et al., 2014), for example, estimates in the USA for indirect costs caused by obesity was US\$ 190.2 billion per year (Cawley and Meyerhoefer, 2012).

Few clinical studies have looked at the effect of different diets on bone morphology. The skeleton acts as a mechanical load bearing structure for the body and achieves this by being a composite tissue made up of many different materials (Rho, et al., 1998). The cells responsible for bone growth and health are osteoblasts (bone growth), osteoclasts (bone resorption) and osteocytes (standard bone cell) (Jiang, et al., 2007). Certain bone

components, such as bone density, muscle attachment size and bone shape are influenced by several genetic and environmental factors such as ethnicity, age, gender, body size and diet (Horlick, et al., 2004; Lac, et al., 2008).

Impact of obesity on living human bone

The question of obesity on bone health is not a new one. Several studies have considered how adipocyte interacts with bone, focusing mainly on identifying the pathways of interaction between adipocyte cells and bone cells such as osteoblasts, osteoclasts and osteocytes (Gimble, et al., 1996; Lecka-Czernik, et al., 1999; Dorheim, et al., 1993; Beresford, et al., 1992). As can be seen in Rosen & Bouxsein (2005) the route mesenchymal stem cell can become either an osteoblast or adipocyte (Figure 1) which means that a slight change in conditions could have a major impact on cell formation of either osteoblasts or adipocytes.

[Figure 1 originally presented here cannot be made freely available via LJMU E-Theses Collection because of copyright. Figure 1 was sourced at Rosen & Bouxsein (2005), Figure 1, Page 37]

Figure 1. Lineage allocation in the bone-marrow milieu (Rosen & Bouxsein, 2005)

Obesity has long been understood to have negative effects on the skeleton. These effects range from changes in overall morphology of bone, bone mineral changes, mechanical property changes (Zernicke, et al., 1995), reduction in cancellous bone (Cao, et al., 2009), increased bone resorption and impaired bone microarchitecture (Patsch, et al., 2011). Zernicke et al. (1995) identified the morphology, mineral and mechanical property changes by studying two groups of rats. The groups consisted of a high-fat sucrose diet (HFS) and a low-fat, complex carbohydrate diet (LFCC). Using these two groups, Zernicke et al. (1995) determined that the femoral necks of the HFS group had smaller cortical shells, larger trabecular cores as well as lower mass-normalised loads, energies and stiffness. These results suggested that the femoral neck of a rodent subjected to a HFS diet may be much less able to deal with sudden changes in loads and could culminate in increased fracture risk.

Alongside the femoral neck, Zernicke et al. (1995) also studied L6 vertebrae and found similar results. The vertebrae of the HFS group had significantly smaller average cross-

sectional areas as well as significantly lower loads, energies and stiffness compared with non-HFS controls. Cao et al. (2009) studied the effect of obesity on bone through two groups of rats. All rats in the study were male and the groups were a standard control and high-fat diet (HFD) group that were both sacrificed after 14 weeks of dietary supplementation. To understand the physical properties of bone in greater detail, both groups were micro-CT scanned and it was determined that tibial trabecular bone volume was reduced and trabecular separation was higher in the HFD group. This indicates that there was a decrease in the cancellous bone, caused by high fat diets in a rodent model. Patsch et al. (2011) also backs up the concept of cancellous bone loss in their findings. The models involved in the Patsch et al. (2011) study included a standard control group which received a low-fat diet, the second group was a standard high fat diet group and the third group was subjected to a low fat diet and switched to high fat three weeks before sacrifice. Both groups 2 and 3 showed signs of bone loss after sacrifice, showing that the changes to bone can occur much more rapidly than previously reported.

Despite the data presented above, not all of the effects of obesity are negative, as in the case of osteoporosis. For example, obesity is said to be a protective factor for reducing fracture risk in osteoporotic individuals (Melton, et al., 2008) and several studies link low BMI to a higher fracture risk (De Laet, et al., 2005; Thomas and Burguera., 2002; Pocock, et al., 1989; Slemenda, et al., 1990; Felson, et al., 1993). However, this view is opposed by a study that appears to show low BMI as an individual risk and any higher body mass as having no effect on fracture risk (Kanis, et al., 2005). Fracture risk is determined by measuring bone mineral density (BMD) using dual energy X-ray absorptiometry (DXA) and is preferentially carried out on the proximal femur (Kanis, 2002). A BMD below 2.5 is considered osteoporotic and the same value is used for both men and women (Kanis, 2002). The concept of obesity being a protective factor against osteoporosis was based on biomechanical theories that a larger body mass would require a stronger support, therefore increasing bone density. However, new research has shown that obesity may be increasing BMD as a result of leptin secretion from the adipose tissue, which is a cytokine-like hormone which can influence the growth of bone (Cirmanova, et al., 2008; Hamrick and Ferrari, 2008). Ellis et al. (2003) have shown that even though obesity has a significant impact on bone density, when corrected for height, the difference lessens to a

negligible amount, thus raising a gap in our understanding, warranting further investigation.

Animal models

Animal models are often used to study the effects of obesity for several reasons. The first is that it gives complete control over the effecting factors on the study. For example, Jee and Li (1990) used a rodent experimental model to immobilise the right hind limb of rats to enhance the effect of overloading in the opposite leg. This would also have the effect of showing the impact of disuse on the immobilised legs, meaning that by applying a single factor limitation, you can receive two sets of data to analyse. Animal models are also used when there is a lack of reliable human samples to be used. This is particularly true in the case of biological anthropologists looking to interpret past behaviour through physical changes to bones. The number of sample populations that are fully documented are extremely low and as such, many forms of partially destructive testing such as X-ray and micro-CT scanning are extremely difficult to gain approval for. Animal models can therefore be used to provide baseline results which can be applied to the human setting in order to much better understand and interpret existing data to and assist in experimental protocol for future analysis, therefore minimising the requirement for further animal models. This has been shown to be effective in several other experimental studies where animal bones have been used to infer general qualities in human bones (Villotte, et al., 2010; Lieberman, et al., 2004).

As useful as animal models are, there are issues comparing animal model samples to human samples. For example, the development of chosen study animal can affect the results and the interpretation in comparison to humans due to differences in developmental milestones between the comparative species. A prime example of this is the Wistar rat, one of the most widely used animals for scientific research. The average life expectancy of a laboratory rat is three years and a human is 80 years. The relevancy of the disparity is that without knowing which developmental stage and the time periods of these stages you cannot compare the samples. For example, you cannot compare a three year old Wistar rat to a three year old human, as one is at the end of its life expectancy and the other is a juvenile. Therefore, a simple calculation can be performed to

determine how many 'rat day's' equal 1 human year. $(80 \times 365) / (3 \times 365) = 26.7:1$ (human days : rat days) & $365 / 26.7 = 13.8:1$ (rat days : human years) (Sengupta, 2011). Using the previous calculation, you can see the disparity in developmental stages of the rat compared to the human Table 3 (Sengupta, 2011). As can be seen in Table 3, most the rodent's life cycle is spent in the weaning period, with 42.4 days being equivalent to 1 human year. In comparison, most of a human life cycle is spent in the adult phase.

Table 3: Average age rate conversion between Rat and human, based on Table found at Sengupta (2011).

Developmental Stage	Rat days : 1 human year
Weaning period	42.4
Prepubescent period	3.3
Adolescent period	10.5
Adult phase	11.8
Aged Phase	17.1
Average	16.4

Aim's and objectives

The aim of this project is to interpret more accurately the effects of body mass and obesity on bone morphology and strength. The results from this study will enhance the interpretation of bones from past populations and aid both paleoanthropologists and biological anthropologists working on archaeological populations. In addition, the study is relevant to the understanding of the acute vs chronic effects obesity has on bone.

The aims of the study are below:

- To form initial insights into how obesity affects bone health during development using varied methodologies and techniques.
- To understand how different scientific fields can be used to answer complex questions in a simplified way.
- To further understand the effect of obesity on bone as a tool to identifying obesity in ancient populations. Therefore, understanding how obesity affected society throughout human history and civilisation.
- To identify how obesity affects bone during developmental periods as an aid for understanding modern day societal pressures of obesity.

The objectives of the study are below:

- Data sets from linear measurements (LM), geometric morphometric shape analysis (GMSA) and cross-sectional shape analysis (CSSA) will be analysed to determine if there are significant differences between obese (CO), control (CC) and calorie restricted (RE) groups.
- To identify the key differences in bone due to obesity from LM, GMSA and CSSA
- To compare and contrast the results (LM, GMSA and CSSA) and identify common patterns.
- To determine whether changes to bone due to obesity are permanent or temporary by comparing RE to both CC and CO.

Materials and Methods

Animals and experimental design

For this study bone samples and wild type Wistar rat (*Ratus norvegicus*) carcasses were kindly donated by the Nutrition and Obesity Research Group (University of Basque Country) who purchased the rats from Harlen Iberica (Barcelona, Spain). The total donated sample consisted of 54 rats in 6 different groups (n=9 rats/group), However this study only used three groups (N=27). Each group was subjected to a different dietary treatment while activity was limited throughout the study by the use of metabolic cages. A metabolic cage is an unstimulated environment that can monitor different environmental conditions such as temperature, respiration, fluid intake, or fluid evacuation. Therefore, these cages are highly valuable where conditions need to be monitored closely over a period of time. The groups were: 1) lean, well-nourished rats (control); 2) high-fat, high-sucrose diet induced obesity adults; and 3) diet-induced obesity rats subjected to caloric restriction. The timeline for the samples and the dietary conditions they were exposed to can be seen in Figure 2 and Table 4. The body mass of each sample can be found in Table 5.

Group	Weeks: 1-5	Weeks: 6-12	Weeks: 13-17
1 – Control (CC)	Green	Yellow	
Juvenile (HFDJ)	Green	Red	
2 - High Fat (CO)	Green	Red	
3 - Calorie restricted (CR)	Green	Red	Yellow
High Fat with Resveratrol (RSV)	Green	Purple	
Calorie Restricted with Resveratrol (R+R)	Green	Red	Brown

Green = weaning, Yellow = standard low energy lean diet, Red = High fat diet, Purple = high fat diet with resveratrol, Brown = standard low energy lean diet with resveratrol. Groups with a number and highlighted in bold are used in this study.

Figure 2: Group name and dietary conditions for each experimental stage in weeks.

Table 4: Diet composition of the Wistar rats fed by the Basque University throughout the experiment.

	HFHS diet	STD diet
Total energy (kcal/g)	4.7	3.9
Composition by energy (%):		
Carbohydrates	35	64
Proteins	20	20
Lipids	45	16

HFHS: High-fat high-sucrose; STD: standard High-fat high-sucrose diet: HFHS diet (OpenSource Diets, Denmark; Ref. D12451)

Standard diet: semi-purified standard diet (OpenSource Diets, Denmark; D10012G).

Table 5: Body mass in grams of all rodents after sacrifice separated by group.

Sample	CC	CO	HFDJ	R+R	RES	RSV
1	413	513	395	429	446	456
2	419	493	427	428	420	463
3	425	475	382	404	426	460
4	459	490	392	410	413	463
5	412	464	303	422	433	433
6	424	445	347	414	413	437
7	413	466	373	402	400	445
8	407	428	386	378	397	388
9	363	461	341	411	394	385

CC = Control, CO = Obese, HFDJ = High Fat Diet Juvenile, R+R = Calorie Restricted and Resveratrol, RES = Calorie restricted, RSV = High Fat Diet and Resveratrol.

Group 1 (CC) were the control group and act as the baseline for all other groups to be measured against. This group were fed a standard diet after being weaned and until they were sacrificed. Group 2 (CO) were fed a high-fat diet for 12 weeks after weaning. Group 3 (RES) was used to help understand the impact of weight loss and to understand if changes caused by obesity were reversible, and if so, what were the signs that identify them. After weaning group 3 (RES) was subjected to a 6-week high-fat diet *ad libitum*

followed by 6 weeks during which they were given the same standard lean diet as given to group 1 (CC). All of the groups were raised in metabolic cages so that activity could be limited, in order to isolate the factor of activity in this experiment. This is of great importance as to fully understand the changes caused by obesity we must limit the influencing factor of muscle strain on bone. The rats were sacrificed at 17 weeks of age; by this age all epiphyses will have been fused, indicating skeletal maturity.

Sample preparation and transportation

After sacrifice at the university in Basque Country by the Nutrition and Obesity Research Group the samples were relieved of visceral fat and intestines by dissection for analysis. After this process was completed, the rodents were wrapped and placed in cool boxes to be transported to Liverpool John Moores University within twenty-four hours of sacrifice. This process was designed to minimise the damage of natural decay or freezing to the carcasses before they could be micro-CT scanned at the MXIF facility at Manchester University. As the sample preparation was time critical, after the micro-CT had been performed the samples were transported back to Liverpool John Moores University for dissection before freezing in -80°C for further analysis.

Micro-CT

Before any samples were removed, all 54 rats were micro-CT scanned at the Manchester X-ray Imaging Facility (MXIF) within 48 hours of being sacrificed. Whole rat carcasses were scanned by micro-CT (Nikon Custom bay, MXIF, Manchester, United Kingdom), at a 0.1182mm resolution using integration time of 500ms, energy of 65Kv and intensity of 330 μA over 2000 projections all from a tungsten x-ray source. Some scans contained a single rat, whereas others contained up to three rats. The rats were placed in clear plastic zip lock bags for health and safety reasons, then wrapped in low density foam to hold the rat in shape as they were scanned. The rats were then placed in polystyrene boxes in a vertical position to reduce the penetration requirements of the scan. Reconstruction was performed by CTpro v2.2 Software.

Dissection

After the micro-CT, the samples were returned to Liverpool John Moores University where a further dissection was performed (Figure 3), secondary to the dissection by the Nutrition and Obesity Research Group at the University of the Basque Country.

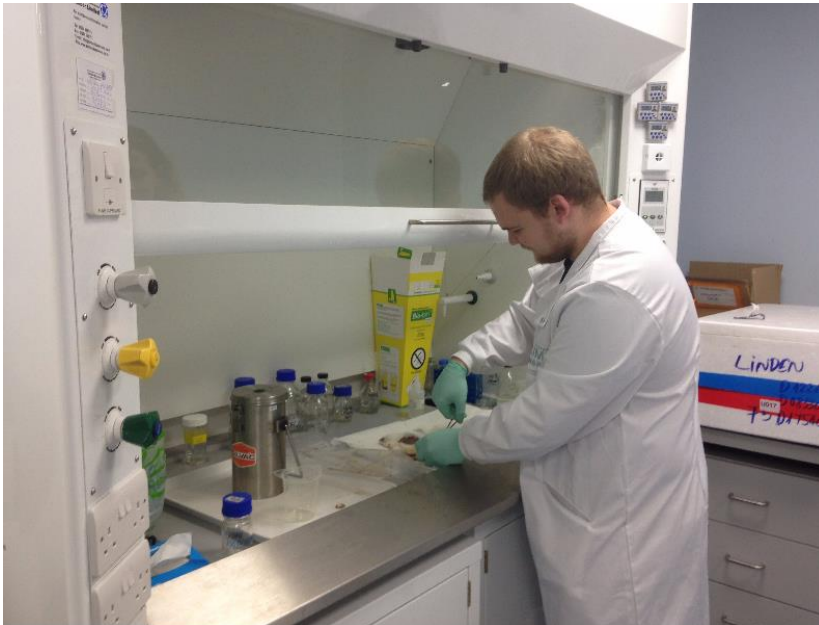


Figure 3 – Dissection of Wistar rat taking place at Liverpool John Moores University

This dissection removed the quadriceps, skin, hair, right femora and brains of all the rodents. These samples were stored at -80C to be used in future analytical projects in order to further build our understanding of obesity on health in general.

Measurement acquisition

Segmentation and alignment

All femora had to be segmented and aligned to the global axis in Avizo 9 software to ensure that the cross-sectional and landmark data collected were accurate and repeatable. Therefore, an intra-observer error test was performed on all types of analysis to ensure that data collection was accurate and replicable. First the microCT scans had to be reconstructed. This is a mathematical process that generates images from X-ray projection data that is obtained at many different angles around the scanned object. This reconstruction is crucial for the acquisition of high quality images and reduce noise and increase spatial resolution and accuracy of the measurements (Figure 4) and relies on

quality and contrast of the original scans. This process was performed at the MXIF facility using CT Pro software.

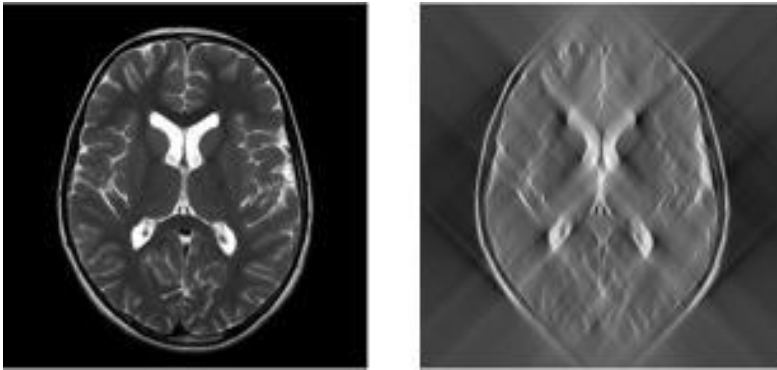


Figure 4: Reconstruction of CT scans is crucial for image accuracy and clarity. First image is properly reconstructed, second shows artifacts due to faulty reconstruction (Image by Frikel and Quinto available on <http://iopscience.iop.org>).

After reconstruction of the CT scans, we were left with the entire skeleton to analyse (Figure 5). In order to simplify the data and also create file sizes that are manageable, segmentation was performed on the area of focus. Segmentation is the process of going through each slice of the scan and manually highlighting the area of interest.

Segmentation, as described above is used to reduce file sizes, but is also a useful tool for density analysis. This is due to segmentation relying on scan density to identify and isolate areas of the scan. More than one layer can be added to the segmentation, meaning that density distribution of the sample of interest can be effectively studied in greater detail.



Figure 5 – Full body micro-CT scan volume render of RE1.

After segmentation was completed, we were left with an isolated virtual image that had no alignment information. Therefore, a global alignment needed to be performed so that all of the segmentation files were aligned in exactly the same way. This alignment finds the centroid of each segmented scan and aligns accordingly (Figure 6).

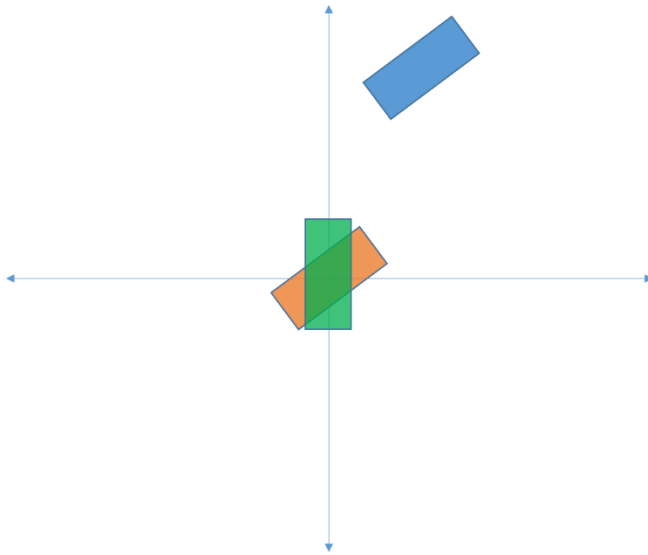


Figure 6 – Diagram of segmentation alignment. Blue rectangle shows the original segmented femur. Orange rectangle shows the 3D co-ordinates of the femur being set to 0. Green rectangle shows the global alignment using the long axis through the centroid of the femoral diaphysis.

Without the global alignment of the segmented files, they cannot be directly compared for analysis beyond linear measurements. For example, the cross section of a horizontal and vertical bone will be non-comparable (Figure 7). Also, a key feature of this step is to ensure that all results are reliable and replicable.

An error test was performed to ensure data collection was reliable and replicable. However, this process took refining and two previous error tests in order to achieve a level of accuracy (5% variance) that was deemed acceptable. The initial challenges faced here was how to globally align the sample to ensure that the bone always aligned in the same way. After overcoming this, the clipping planes used for placing landmarks needed to be aligned accurately with the global alignment of the segmented bone. This process

was potentially the most important process of the entire experiment, as any inaccuracies made here could have a huge impact on further results that would not be identifiable and would appear anomalous.

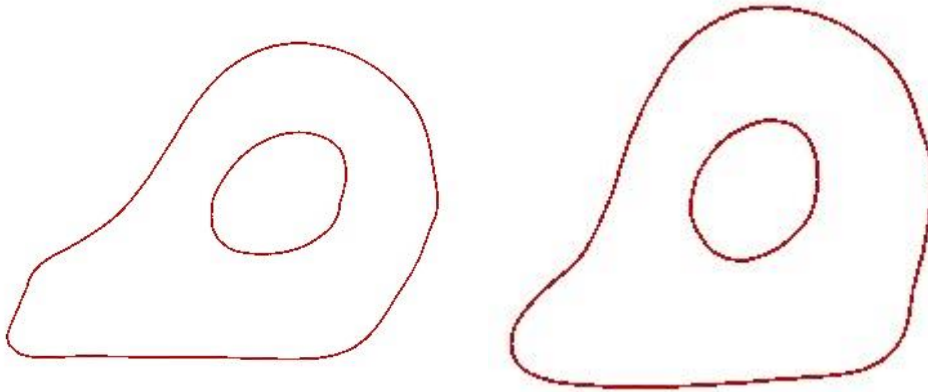


Figure 7 – The left cross-section is correctly aligned compared to the right cross-section which was taken from the un-aligned femur and is therefore oblique to the long axis. The cross-sectional analyses of these slices would be different and highlights the importance of correct alignment.

Linear Measurements

The first step in identifying bone differences between groups was using linear measurements. Linear measurements are both simple and effective for characterisation certain aspects such as length, width and circumference.

The measurements were taken using landmarks on the virtual representations of the microCT scanned bones. The measurements that were taken in this study were as follows: maximum length, distal epiphysis width, distal epiphysis diameter, distal epicondyle width and the epiphysis/epicondyle width ratio. Definitions for the measurements are available in Table 6 and Figure 8. These measurements were chosen as they would best represent the effect of weight loading through the bone and the effect of increased weight of the body around the epiphysis. The epiphysis diameter was not directly measured but calculated using the width as if the diameter would replicate that of a circle by using the equation: Circumference = Diameter * Pi.

Table 6 – Description of Linear Measurements

Measurement	Definition
Maximum Length	The length from the most superior to the most inferior point of the femur
Distal Epiphysis Diameter	The diameter of the epiphysis in the medio-lateral direction
Distal Epiphysis Circumference	The circumference of the epiphysis, calculated using the equation $\pi \times \text{Diameter}$.
Epicondyle width	The width of the two most inferior points of the epicondyle's
Epiphysis/Epicondyle width ratio	The ratio between the epiphysis diameter and epicondyle width.

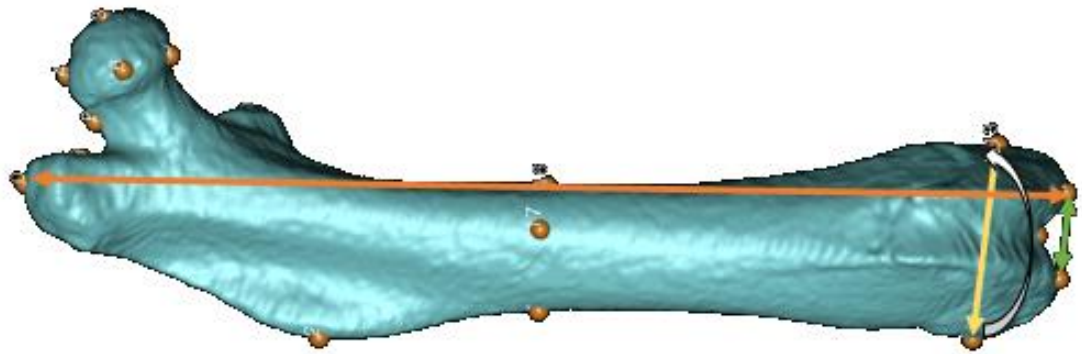


Figure 8 – representation of the Linear measurements taken on segmented Femur. Maximum Length is the orange arrow, epiphysis diameter is yellow, epiphysis circumference is white and epicondyle width is green.

Data analyses

Geometric Morphometric Shape Analysis

In addition to the linear measurements, eighteen three-dimensional (3D) landmarks were collected to define the overall shape of the femur irrespective of size (Table 7). All landmarks were collected using Avizo 9 software on segmented and aligned models (Figure 9). In order to accurately take landmarks and ensure they were repeatable, three clipping planes were created in the X, Y and Z axis. Using these clipping planes allows easy and accurate location of all landmarks that were chosen for the analysis. After landmarks have been placed, the locations of these can be exported in xyz coordinates. The coordinates of each landmark can then be used to calculate lengths between pre-defined landmarks. These landmarks were used as they best define the shape of the bone for geometric morphometric shape analysis while also allowing for clearly defined locations to be identified for linear measurements.

Using software package MorphoJ, the landmarks were corrected for size by use of Procrustes fit followed by a PCA. As previously mentioned, the Procrustes fit is used to remove the effects of size from the sample (Adams, et al., 2004). The principle component analysis reduces the dimensionality of the data while maintaining the variability, allowing for covariance and correlation tests to be performed on the data (Jolliffe, 2014).

Table 7 – definition of landmarks placed on the femur

Order of Placement	Landmark	Landmark Abbreviation	Definition
1	Superior Greater Trochanter	SGT	The most superior point of the greater trochanter
2	Inferior Medial Condyle	IMC	The most distal point of the medial condyle
3	Lateral Third Trochanter	LTT	The most lateral point of the third trochanter.
4	Fovea Capitis	FC	The site of ligament attachment on the femoral head.
5	Superior Femoral Head	SFH	The most superior point on the femoral head
6	Inferior Femoral Head	IFH	The most inferior point on the femoral head
7	Anterior Femoral Head	AFH	The most anterior point on the femoral head
8	Posterior Femoral Head	PFH	The most posterior point on the femoral head
9	Medial Femoral Neck	MFN	The most medial point on the femoral neck along the superior surface
10	Distal Femoral Neck	DFN	The most distal point on the femoral neck along the superior surface
11	Posterior Lesser Trochanter	PLT	The most posterior point on the lesser trochanter
12	Lateral Lateral Condyle	LLC	The most Lateral point on the Lateral condyle
13	Medial Medial Condyle	MMC	The most medial point on the medial condyle
14	Inferior Lateral Condyle	ILC	The most inferior point on the Lateral Condyle
15	Mid-section Lateral	MSL	The most lateral point of the mid-section
16	Mid-section Medial	MSM	The most medial point of the mid-section
17	Mid-section Anterior	MSA	The most anterior point of the mid-section
18	Mid-section Posterior	MSP	The most posterior point of the mid-section

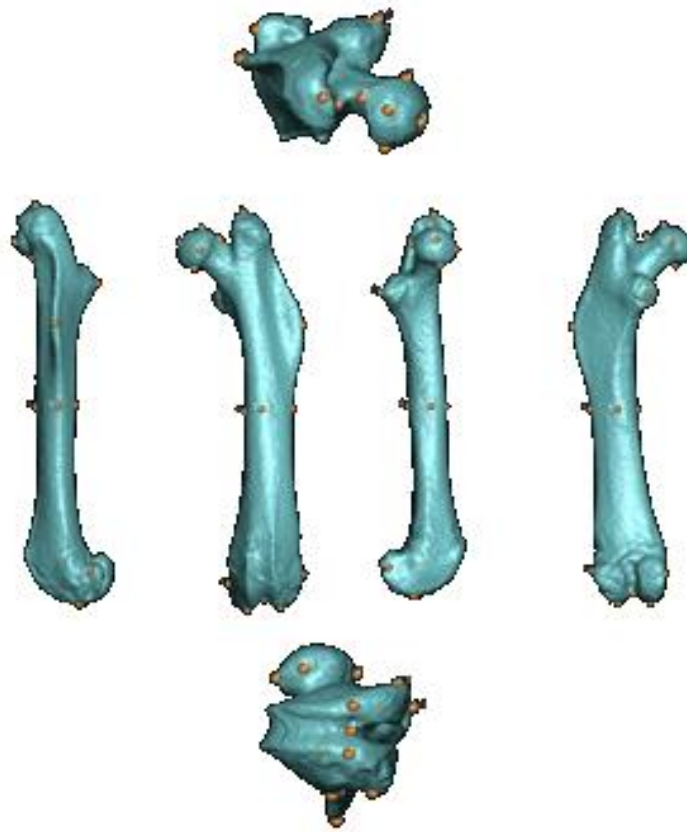


Figure 9 – Segmented femur in all planes displaying all landmark positions

Cross-sectional Shape Analysis

After the shape was analysed, the biomechanical properties of bone needed to be understood. To do this, a cross-section was taken from two locations, midshaft and the most lateral point of the third trochanter. The midshaft is the traditional location of cross-sectional analysis as it is seen as the weakest point of the shaft and is also easily identified by metric analysis on all long bones. However, to further understand the influence of obesity on enthesal development the third trochanter was used. The third trochanter is the largest muscle attachment site on the femoral shaft of the rat and therefore should show the plastic reaction of bone cause by muscle. The cross-sections were processed to ensure that they met the requirements for the moment macro to calculate the biomechanical properties of each individual rat (John Hopkins School of Medicine, 2015). The biomechanical properties are presented in Table 8. The moment macro was then

calculated the biomechanical variables as previously discussed. All measurements were then corrected for body mass and bone length to remove any size bias from the statistical analysis (Prentice, et al., 1994).

Table 8 – Definitions of the biomechanical properties used in Cross sectional shape analysis.

Abbreviation	Definition
TA	Total area of bone
CA	Total cortical area of bone
MA	Total medullary area of bone. Calculated as TA-CA.
Xbar	The new section centroid in the medio-lateral plane
Ybar	The new section centroid in the antero-posterior plane
Ix	Bending rigidity in the x-axis (medio-lateral)
Iy	Bending rigidity in the y-axis (anterio-posterior)
I _{max}	Maximum bending rigidity found in any plane
I _{min}	Minimum bending rigidity found in any plane
I _{max} /I _{min}	The ratio of I _{max} and I _{min}
Theta	The angle of bone rotation from the centroid
J	Polar second moment of area (overall strength of bone)
Z _x	Section modulus of bone in the x-axis (medio-lateral)
Z _y	Section modulus of bone in the y-axis (anterio-posterior)
Z _p	Overall section modulus of bone
MaxXrad	The maximum length between the cortical exterior in the medio-lateral plane
MaxYrad	The maximum length between the cortical exterior in the antero-posterior plane
MaxRad	The maximum length between the cortical exterior of the bone in any plane.

Discriminant function analysis was performed to see which measurements could be used to correctly classify the groups. This cross-sectional method has been successfully used by myself to estimate sex from the clavicle and predict the contribution of activity to this sex

estimation. This work built upon my undergraduate project and was submitted and accepted for publication in the journal *Homo* during my MPhil (Atterton, et al, 2016).

Statistical analyses

An ANOVA was used to identify which linear measurements were significantly different between Group 1 control (CO), Group 2 obese (CO) and Group 3 restricted (RE). In order to further understand the differences between the groups, post-hoc Bonferroni tests were carried out. To further understand the classification power of the linear measurements, a Discriminant Function Analysis (DFA) was performed between all three groups.

GMSA uses the landmarks pre-defined in Table 7 to express the overall shape of the bone in a virtual environment with the effect of size removed.

The cross-sectional properties were first analysed for all three groups together using Discriminant Function Analysis. An ANOVA was also performed at each cross-section location between all three groups.

To understand in more detail what effect each treatment was having on the cross-sectional biomechanical properties, Discriminant Function Analyses and independent t-tests were carried out two groups at a time: between control and obese, control and calorie restricted and obese and calorie restricted groups.

Regression analyses were used to test for the effect of the biomechanical properties on weight.

All analyses were carried out in SPSS 21.

Results

Linear measurement comparisons

All Linear measurements were significantly different between the control (CO), obese (CO) and restricted (RE) groups; maximum length [$F(2,24) = 5.271, p = 0.013$], epiphysis diameter [$F(2,24) = 10.176, p < 0.001$], epiphysis circumference [$F(2,24) = 10.176, p < 0.001$], epicondyle width [$F(2,24) = 5.262, p = 0.013$] and epiphysis/epicondyle width ratio [$F(2,24) = 4.170, p = 0.028$]. For maximum length, there is a significant difference between control (CC) and obese (CO) ($p=0.014$) illustrated in Figure 10, with the obese bones being longer than the control. The restricted group showed greater variability and were not significantly different from the obese or control groups. There were also differences between control-obese and obese-restricted ($p<0.001$ and $p=0.015$ respectively) for distal epiphysis diameter and also epiphysis circumference ($p<0.001$ and $p=0.015$ respectively) which can be seen in Figures 11 and 12, and in both cases, control femora were found to be larger than the obese. As seen in Figure 13, the epicondyle width measurement was significantly different between control and restricted groups (RE) ($p=0.012$), with control being larger than the restricted group. The same groups were also significantly different for the epiphysis/epicondyle ratio ($p=0.024$) (Figure 14), with restricted having a larger ratio than control.

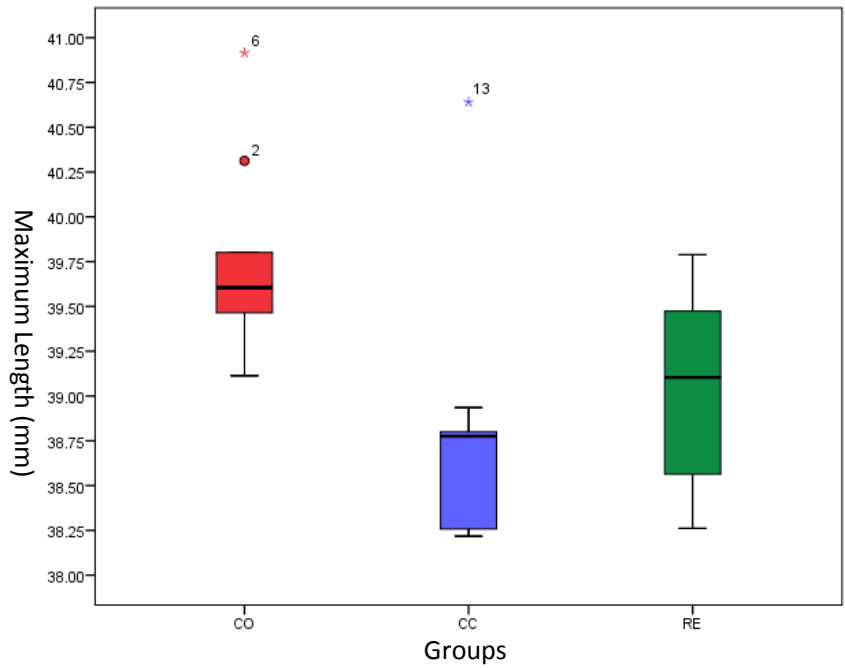


Figure 10: Difference between control group (CC blue), obese group (CO red) and calorie restricted group (RE green) in maximum femoral length.

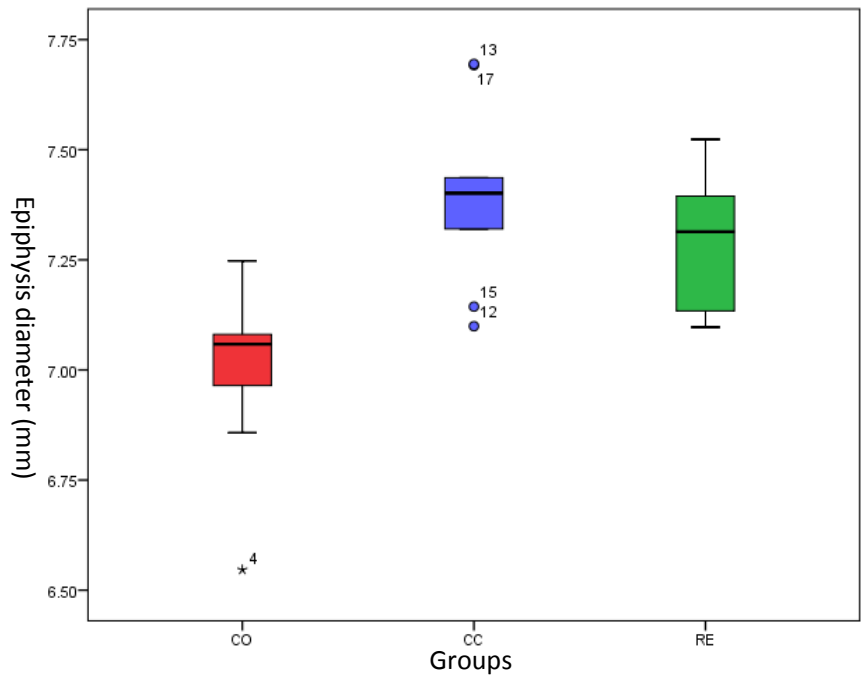


Figure 11: Differences between control group (CC blue), obese group (CO red) and calorie restricted group (RE green) in the femoral epiphysis diameter measurement.

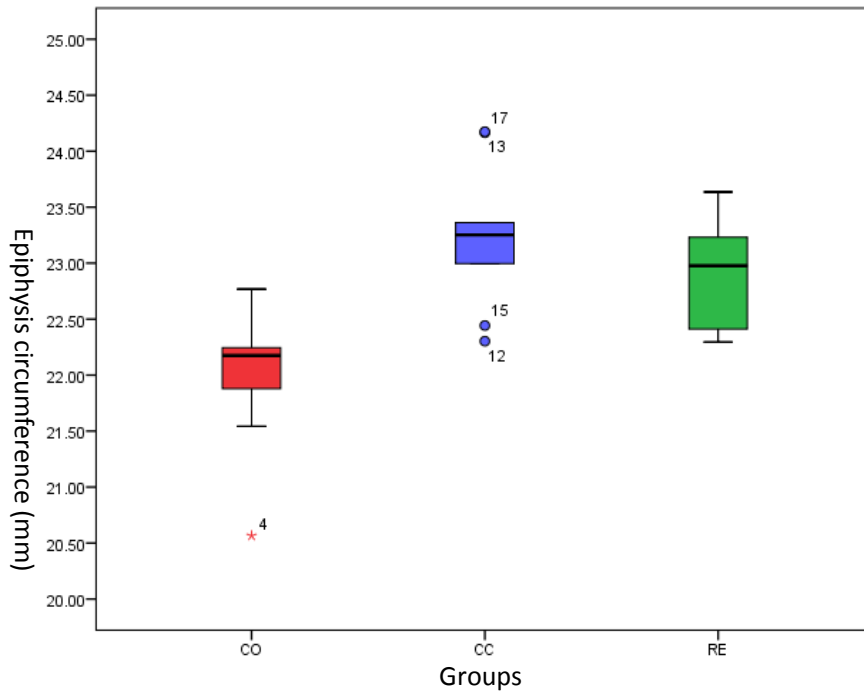


Figure 12: Differences between three groups (X-axis); control group (CC blue), obese group (CO red) and calorie restricted group (RE green) for the epiphysis circumference (Y-axis).

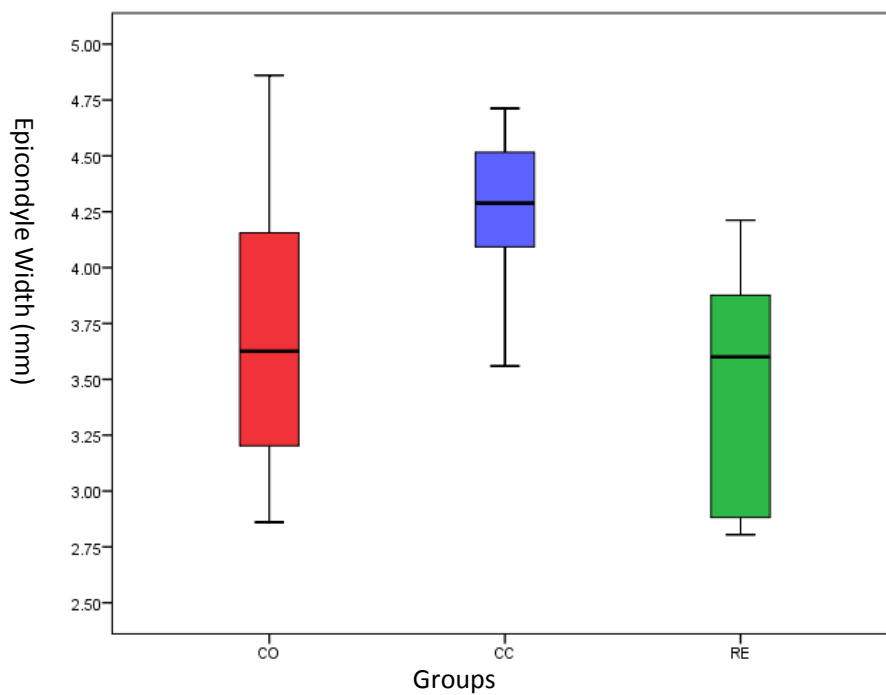


Figure 13: Differences between three groups (X-axis); control group (CC blue), obese group (CO red) and calorie restricted group (RE green) for the Epicondyle width (Y-axis).

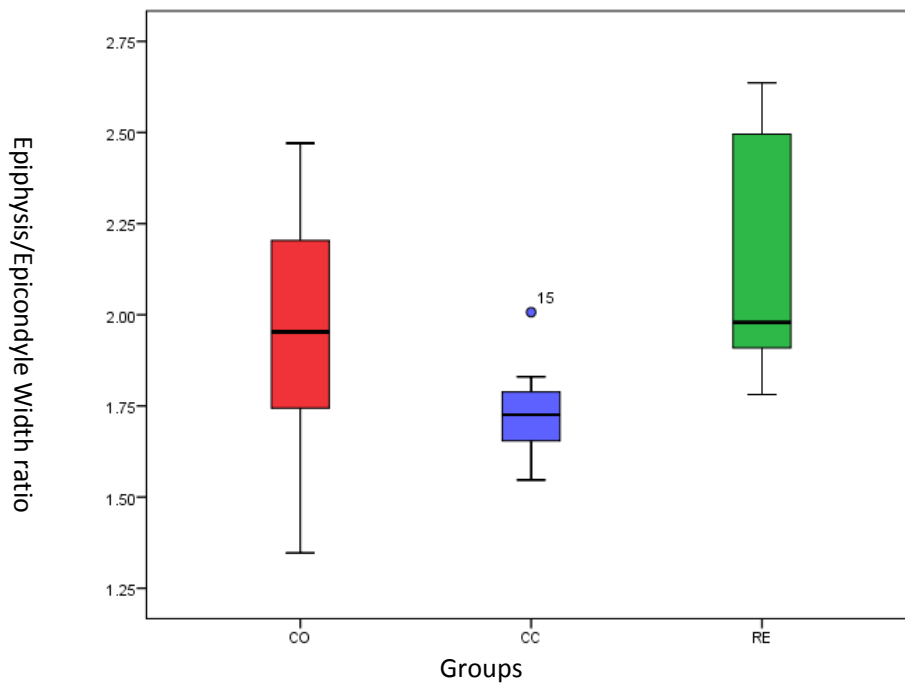


Figure 14: Differences between three groups (X-axis); control group (CC blue), obese group (CC red) and calorie restricted group (RE green) for the Epiphysis/Epicondyle width ratio (Y-axis).

During the DFA all measurements were included in the analysis except epiphysis width. The DFA correctly classified 81.5% (Figure 15) with cross-validation of 66.7%. Two discriminant functions were used to classify the measurements. The first explained 87.7% of variance, canonical $R^2=0.821$ and the second explained 12.3% of variance, canonical $R^2=0.474$. For function 1 through 2, significant differences were identified between all three groups, with $\Lambda=0.252$, $\chi^2(8)=31.012$ and $p<0.001$. However, there were no more significant differences found with more than two functions between all three groups, with $\Lambda=0.775$, $\chi^2(3)=5.736$ and $p=0.125$.

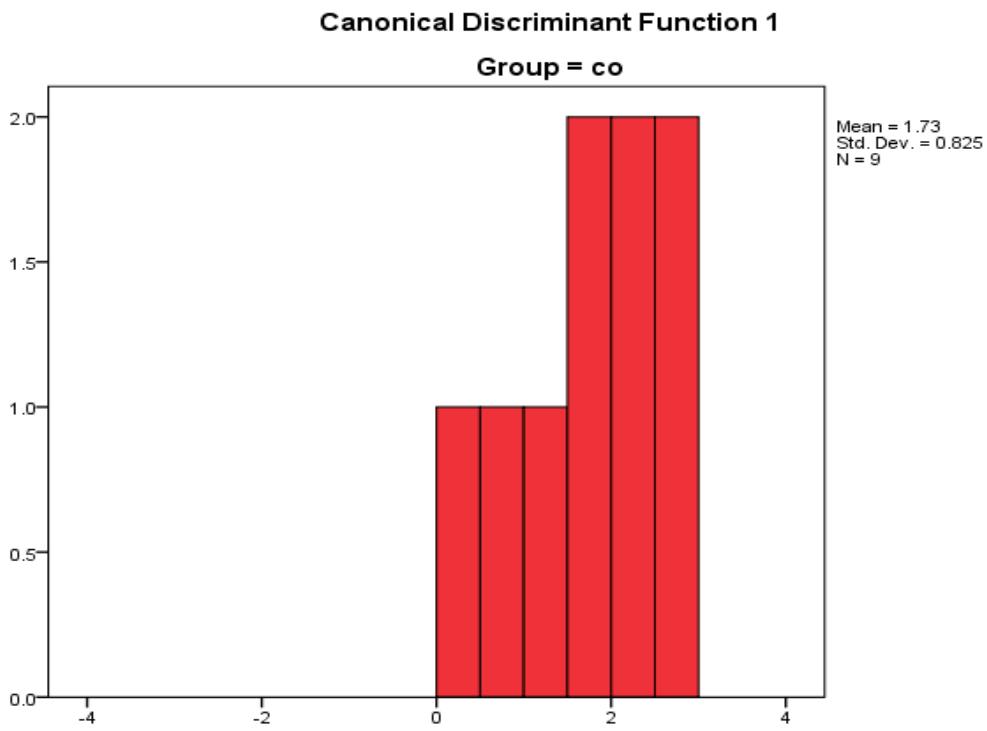
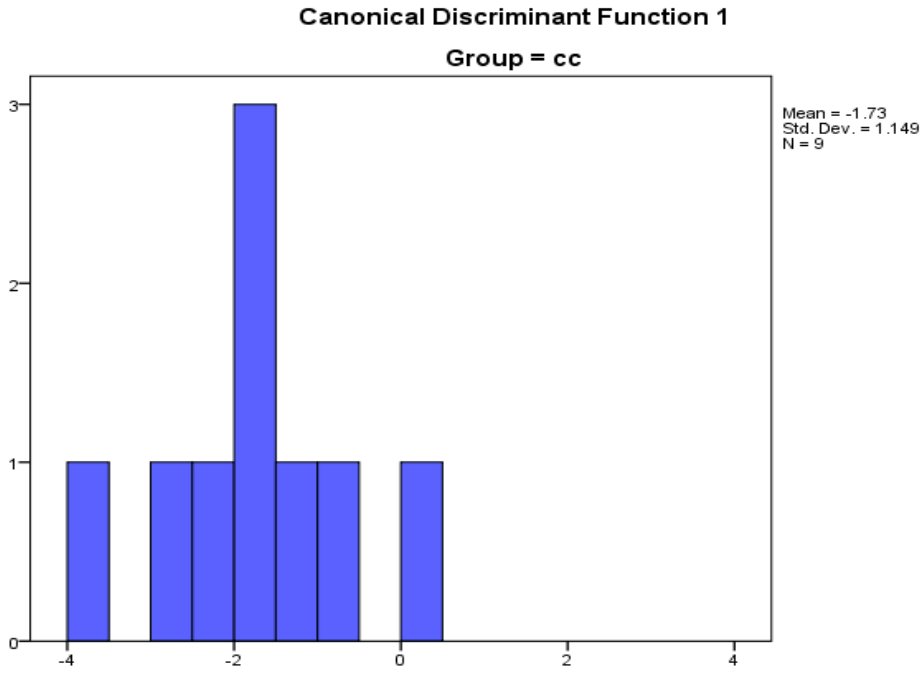


Figure 16: Distribution of the control group (CC blue) and the obese group (CO red), from the linear measurements discriminant function analysis. Values greater than 0 were classified as obese and values less than 0 were classified as non-obese.

There was only one discriminant function required to successfully classify between the two groups, explaining 100% of the variance, canonical $R^2=0.878$. There were significant difference between control and obese groups found during the classification, with $\Lambda=0.229$, $\chi^2(4)=20.610$ and $p<0.001$. The most discriminating measurement was maximum length (function coefficient=1.139) followed by epiphysis diameter (function coefficient=-5.052), then epicondyle width (function coefficient=0.643) and finally epiphysis/epicondyle width ratio (function coefficient=3.626). Using this information, the following equation can be used to discriminate between obese and non-obese groups with 94.4% accuracy.

$$(\text{Maximum length} * 1.139) + (\text{Epiphysis diameter} * -5.032) + (\text{Epicondyle width} * 0.643) + (\text{Epiphysis/Epicondyle width ratio} * 3.626) - 17.575 = X$$

If $X < 0$ then the individual was classified as non-obese and if $X > 0$ the individual was classified as obese (Figure 16).

Geometric morphometric shape analyses

The overall distribution between the two main principle shape components can be seen in Figure 17. PC1 separates the control group from the obese and calorie restricted groups and PC2 separates the obese and calorie restricted groups. The shape difference observed can be seen in Figure's 18 and 19. Figure 18 shows the shape of the control individual located on the most positive location on the graph (scale factor = +0.04) and shape of the obese individual located on the most negative location on the graph (scale factor -0.02). The shape changes identified were a shortening and widening of the distal epiphysis alongside thinning of the femoral neck. Figure 19 shows the most extreme positive obese shape (scale factor = 0.02) and calorie restricted shape (scale factor = -0.03). The shape change identified on PC2 was the relative height of the third trochanter. PC1 explains 41% of the total shape variance and PC 2 Explains 11% of shape variance (Figure 20).

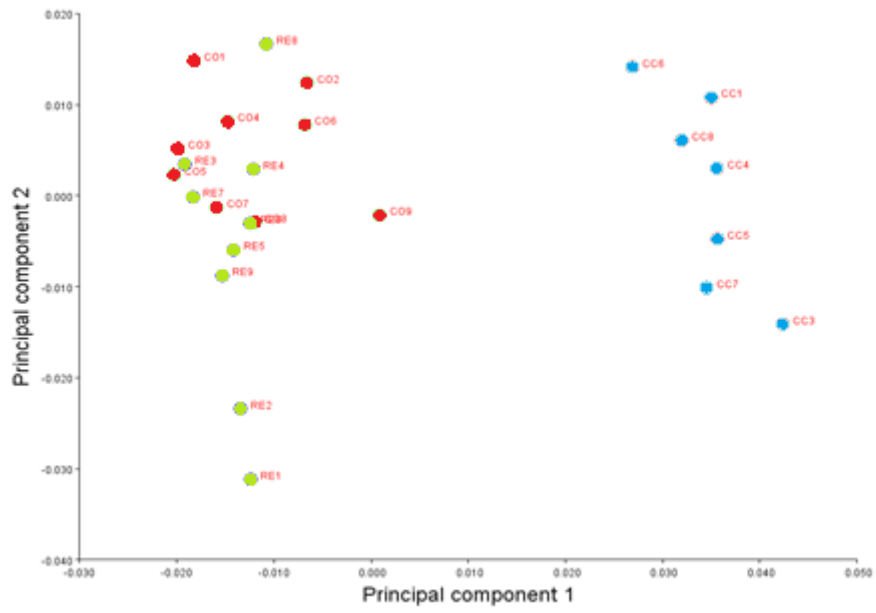


Figure 17: Principal component's graph, displaying the distribution of the three groups; control (CC blue), Obese (CO red) and Calorie restricted (RE green).

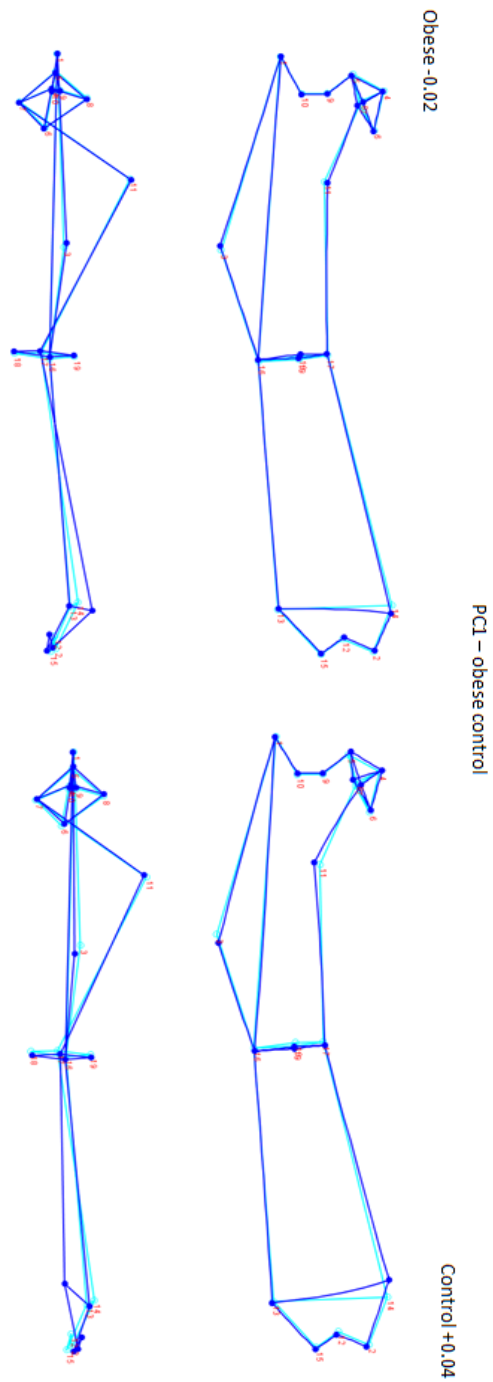


Figure 18: Overall shape changes for principal component 1 between control and obese groups. The light blue line defines the average shape, and the dark blue the extent of shape change caused by PC1.

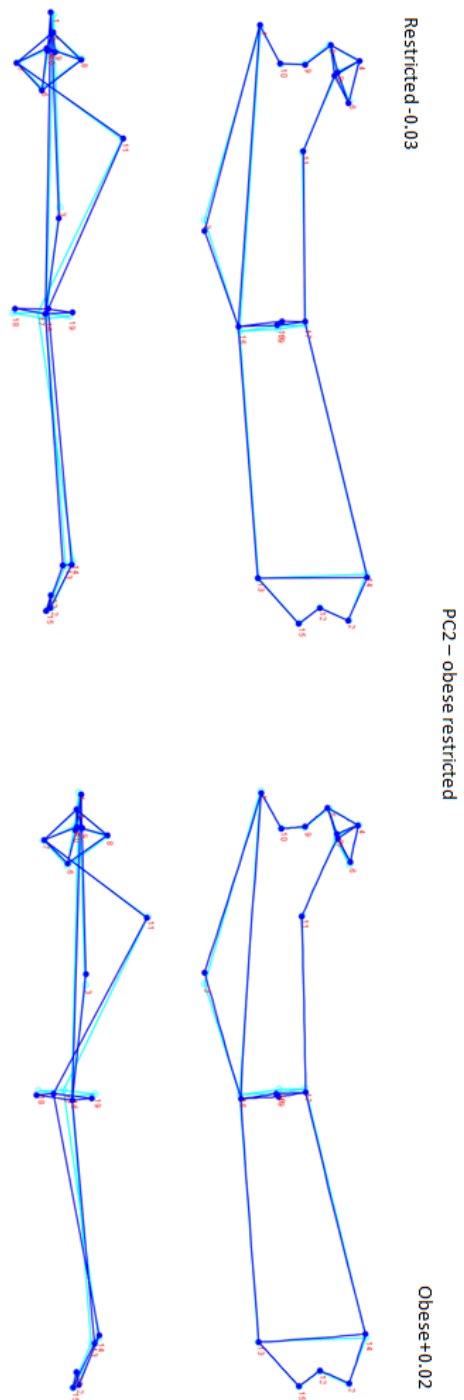


Figure 19: Overall shape changes for principal component 2 between obese and calorie restricted groups. The light blue line defines the average shape, and the dark blue the extent of shape change caused by PC2.

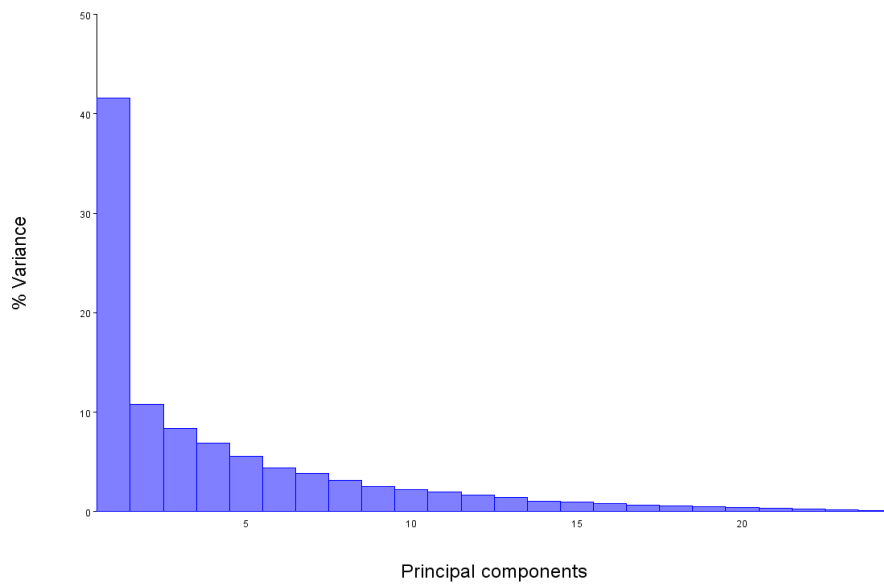


Figure 20: Principal component (X-axis) compared against total % variance (Y-axis) explained by each principal component.

Cross-sectional shape analyses

The initial discriminant function tests were performed on both the midshaft and trochanter using all three groups (Figures 21 and 22) and the cross-sectional measures described above. At the midshaft, 73.1% of cases were correctly classified, but the cross-validation was very poor at only 46.2%. A similar set of results was obtained from the trochanter with 91.3% of cases correctly classified but with only 39.1% of cases cross-validated (Table 9). Both discriminant functions required two steps to reach 100% of variance explained. For the trochanter 94.2% of variation was explained by function one and 5.8% explained by function 2 compared with at the midshaft where 80.2% of variance is explained by function 1 and 19.8% by function 2 (Table 10). The factors that were used in each function for each section can be seen in Table 11.

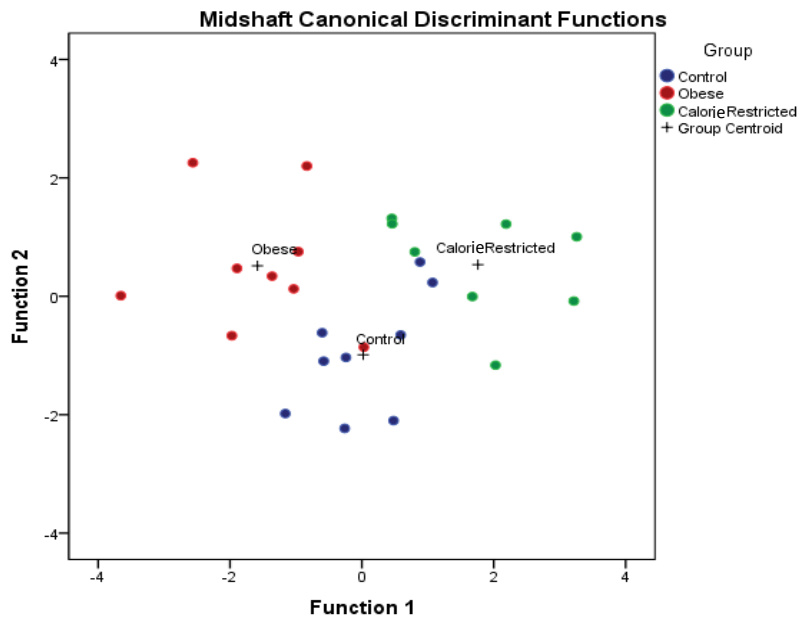


Figure 21: Overall distribution of the three groups; control (CC blue), obese (CO red) and calorie restricted (RE green), from the cross-sectional shape discriminant function analysis at the Midshaft location.

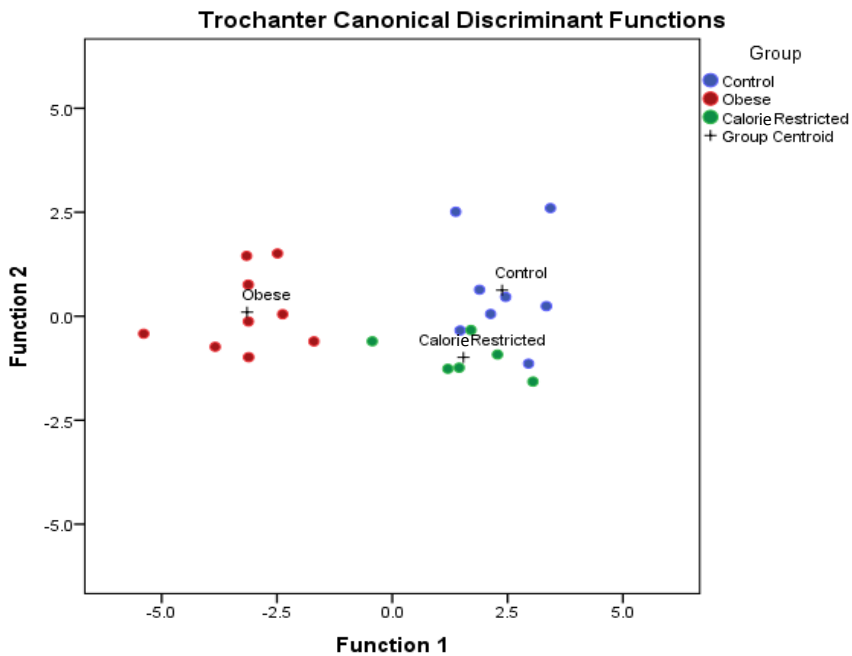


Figure 22: Overall distribution of the three groups; control (CC blue), obese (CO red) and calorie restricted (RE green), from the cross-sectional shape discriminant function analysis at the trochanter location.

Table 9: Discriminant function classification and cross validated classifications for both the midshaft and trochanter.

			Midshaft			Trochanter		
			Control	Obesity	RE	Control	Obesity	RE
Original	Count	Control	8	0	1	6	0	2
		Obesity	2	7	0	0	9	0
		RE	2	1	5	0	0	6
	%	Control	88.9	0	11.1	75	0	25
		Obesity	22.2	77.8	0	0	100	0
		RE	25	12.5	62.5	0	0	100
CV	Count	Control	2	3	4	1	1	6
		Obesity	2	5	2	0	7	2
		RE	4	2	2	5	1	0
	%	Control	22.2	33.3	44.4	12.5	12.5	75
		Obesity	22.2	55.6	22.2	0	77.8	22.2
		RE	50	25	25	83.3	16.7	0

Midshaft: 76.9% original cases correctly classified, 34.6% cross-validated correctly

Trochanter: 91.3% original cases correctly classified, 34.8% cross-validated correctly

Discriminant function results for both the midshaft and trochanter cross-sections. CR = Calorie Restricted, CV = Cross-validated.

Table 10: The discriminant functions used for the factors used in the analysis for both midshaft and trochanter.

Function	Midshaft				Trochanter			
	Eigenvalue	% variance	Cumulative %	Canonical correlation	Eigenvalue	% variance	Cumulative %	Canonical correlation
1	1.086	75.6	75.6	0.722	6.284	93.4	93.4	0.929
2	0.35	24.4	100	0.509	0.442	6.6	100	0.554

Table 11: The standardised Canonical Discriminant Function Coefficients for the factors used in the analysis for both midshaft and trochanter.

	Midshaft Function		Trochanter Function	
	1	2	1	2
lmaxmin	1.418	1.495	3.913	-1.247
MA	1.137	0.385	0.32	-4.716
TA	2.304	5.455	1.849	-14.084
Xbar	-0.244	0.469	0.565	-0.89
Ybar	-0.791	-0.711	0.374	0.919
lx	-2.342	-2.102	-15.539	-4.946
ly	10.018	13.742	8.706	-7.466
Zy	-9.418	-16.768		
Zp	-1.125	-0.33	4.605	25.044
MaxXrad			-4.682	-1.414
MaxYrad			-1.364	-8.980
MaxRad			3.467	21.623

lmaxmin = Ratio of maximum and minimum bending rigidity, MA = Medullary Area, TA = Total Area, Xbar = average dimension size in antero-posterior plane, Ybar = average dimension size in medio-lateral plane, lx = bending rigidity in the antero-posterior plane, ly = bending rigidity in the medio-lateral plane, Zy = bone strength in the medio-lateral plane, Zp = overall bone strength of cross-section, MaxXrad = maximum radial dimension size in the antero-posterior plane, MaxYrad = maximum radial dimension size in the medio-lateral plane, MaxRad = maximum radial dimension in any direction.

The CSSA at the midshaft revealed significant differences for the factors MaxXrad [$F(2, 23) = 4.919, p = 0.017$] and Theta [$F(2, 23) = 6.2, p = 0.007$]. The differences were found between control and obese rats for MaxXrad ($p=0.026$); for Theta, obese animals were different from both control and calorie restricted groups ($p=0.014$ and $p=0.023$ respectively).

At the trochanter, there were significant differences for the same factors (MaxXrad [$F(2, 20) = 8.164, p = 0.003$] and Theta [$F(2, 20) = 6.273, p = 0.008$]). For MaxXrad, differences were observed between the obese group and both the control ($p=0.004$) and the calorie restricted ($p=0.025$). The Theta value was significantly different between the control and obese groups ($p=0.007$).

Control – obese

DFA

At both the midshaft and trochanter 100% of cases were correctly classified with cross-validations of 88.9% and 76.5% respectively. The midshaft and trochanter only had one discriminant function each explaining 100% of variance (midshaft canonical $R^2=0.952$, trochanter canonical $R^2=0.933$). Both locations differentiated significantly between groups, midshaft $\Lambda=0.094, \chi^2(11)=24.874, p=0.01$; trochanter $\Lambda=0.130, \chi^2(9)=21.422, p=0.011$). The factors that had the highest discriminatory power were I_x (midshaft function coefficient = -21.789 and trochanter function coefficient = -11.434) and I_y (midshaft function coefficient = 15.474 and trochanter function coefficient = 15.601).

t-test

With equal variances assumed, the following factors were significantly different at the midshaft; I_{maxmin} [$t(16)=2.206, p=0.042$], MA [$t(16)=2.401, p=0.029$], $Ybar$ [$t(16)=-2.753, p=0.014$] and Θ [$t(16)=2.668, p=0.017$], with all factors being larger in the obese groups. The only factor that was significant when equal variances could not be assumed was MaxXrad [$t(9.335)=-2.785, p=0.013$]. At the trochanter, with equal variances assumed, the following factors were significantly different; $Ybar$ [$t(15)=-2.584, p=0.021$], MaxXrad [$t(15)=-3.733, p=0.002$] and Θ [$t(15)=3.823, p=0.002$], again with the obese groups being the larger.

Control – calorie restricted

DFA

At the midshaft 88.2% of cases were correctly classified with cross validation of 35.3%. Only one discriminant function was needed, explaining 100% of variance, canonical $R^2=0.689$. The midshaft did not significantly differentiate between groups, ($\Lambda=0.525$, $\chi^2(9)=6.77$ $p=0.661$). At the trochanter 92.9% of cases were correctly classified with cross validation of 35.7%. Only one discriminant function was needed, explaining 100% of variance, canonical $R^2=0.823$. The midshaft did not significantly differentiate between groups ($\Lambda=0.323$, $\chi^2(11)=7.349$ $p=0.77$). The factors that had the highest discriminatory power at the midshaft were I_y (function coefficient = 12.736) and Z_y (function coefficient = -8.621). At the trochanter the factors were MaxXrad (function coefficient = 14.138) and MaxYrad (function coefficient = -11.509).

t-test

No values were statistically different when a *t*-test was performed between these groups.

Obese – calorie restricted

DFA

At the midshaft 100% of cases were correctly classified with cross validation of 88.2%. Only one discriminant function was needed, explaining 100% of variance, canonical $R^2=0.96$. The midshaft significantly differentiated between groups, with $\Lambda=0.079$, $\chi^2(11)=24.109$ $p=0.012$. At the trochanter 100% of cases were correctly classified with cross validation of 60%. Only one discriminant function was needed, explaining 100% of variance, canonical $R^2=0.954$. The midshaft significantly differentiated between groups, with $\Lambda=0.089$, $\chi^2(10)=19.31$ $p=0.036$. The factors that had the highest discriminatory power at the midshaft were I_y (function coefficient = -18.363) and MaxXrad (function coefficient = 23.008). At the trochanter the factors were I_x (function coefficient = -18.231) and I_y (function coefficient = 17.627).

t-test

With equal variances assumed, the following factors were significantly different at the midshaft; MaxXrad [$t(13)=2.828$, $p=0.014$] and Ybar [$t(13)=2.826$, $p=0.014$] with the obese groups being larger than the calory controlled. The only factor that was significantly different when equal variances could not be assumed was MaxXrad [$t(9.335)=-2.785$, $p=0.013$] which was larger in the obese group. At the trochanter, with equal variances not assumed, the following factors were significantly different; Ybar [$t(11.136)=2.666$, $p=0.022$] and Theta [$t(8.764)=-2.516$, $p=0.034$], both of which were larger in the obese group.

Body mass Analysis

With equal variances assumed, the obese group was heavier than both the control [$t(16) = -4.658$, $p<0.001$] and calorie restricted groups [$t(16) = -5.281$, $p<0.001$]. However, with equal variances assumed there was no significant differences between control and calorie restricted groups [$t(16) = -0.077$, $p = 0.94$]. All six groups can be seen in Figure 23.

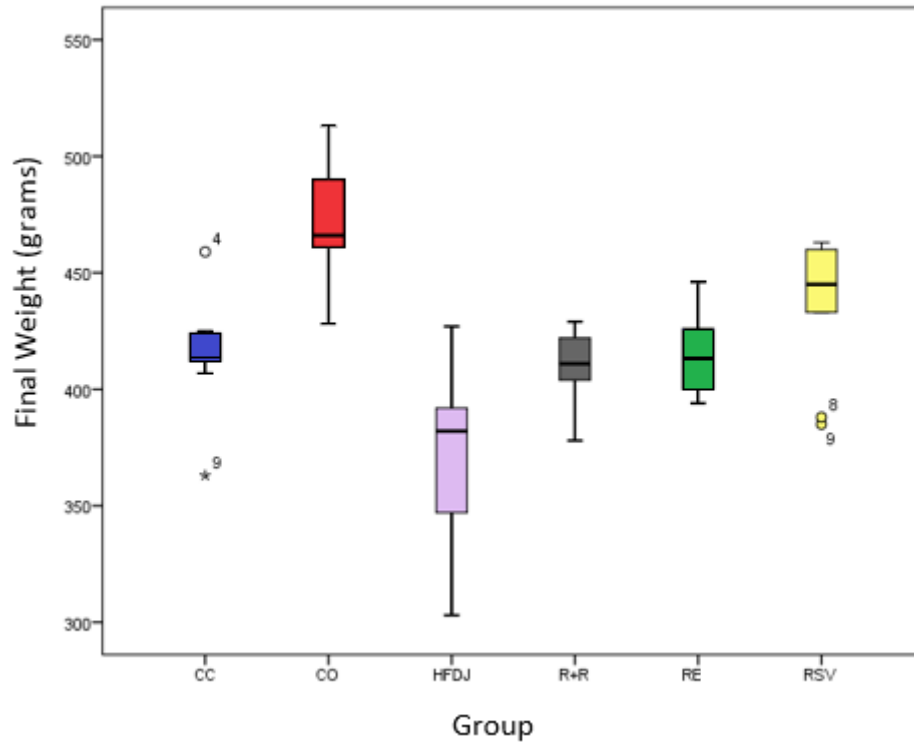


Figure 23: The body mass of all 6 groups, received from the Basque Country University; Control (CC blue), obese (CO red), high fat diet juvenile (HFDJ purple), resveratrol and calorie restricted (R+R grey), calorie restricted (RE green) and resveratrol and high fat diet (RSV yellow).

Following this, a multiple regression was performed between the Cross-sectional shape analysis factors and body mass, to determine if these variables can be used to correctly calculate body mass. The following variables were included in the analysis, however none were significant predictors on their own; MA (Beta = 0.447, $p = 0.310$), TA (Beta = 1.429, $p = 0.370$), Xbar (Beta = 0.053, $p = 0.754$), Ybar (Beta = -0.137, $p = 0.424$), lx (Beta = 7.280, $p = 0.168$), ly (Beta = 9.482, $p = 0.105$), Theta (Beta = -0.240, $p = 0.115$), Zx (Beta = -8.220, $p = 0.273$), Zy (Beta = -14.741, $p = 0.091$), MaxXrad (Beta = -0.851, $p = 0.721$), MaxYrad (Beta = -0.851, $p = 0.721$), Zp (Beta = 0.718, $p = 0.890$), MaxRad (Beta = 0.216, $p = 0.931$) and lmaxmin (Beta = 1.535, $p = 0.394$). Together, however, these variables predicted body mass, $F(14, 11) = 4.787$, $p = 0.006$, $R^2 = 0.859$.

Discussion

The first objective was to determine if there are significant differences between CO, CC and RE groups. This was achieved through use of statistical analysis of all three methodologies data sets. For linear measurements, all three groups were significantly different across all measurements which suggests that linear measurements were effective at distinguishing between all three groups. A single mathematical function (87.7% of variance explained) including maximum length, distal epiphysis width, distal epiphysis diameter, epicondyle width and the epiphysis/epicondyle width ratio could discriminate between the control and obese groups almost perfectly, and a second function (12.3% of variance explained) was required to differentiate between the calorie restricted group and the other two groups. Even more, when the analysis was restricted to the control and obese groups, the resulting function correctly classified 94.4% of cases. The 3D geometric morphometric shape analyses (GMSA) showed that most variance was explained by PC1 (41% variance explained). PC1 distinguished between control and both obese and calorie restricted groups, although not between obese and calorie restricted (Figure 17). The midshaft CSSA discriminant function distribution (Figure 21) showed that the three groups were slightly distinguishable but there was a large amount of overlap. This is shown by the results (76.9% of cases were correctly classified but only 34.6% were cross-validated correctly) suggesting that some of the individuals in the samples optimistically bias the result due to their extreme values. For the trochanter, the obese group was completely separated from the control and calorie restricted, but the calorie restricted and control had slight crossover (Figure 22).

The second and third objective are intrinsically linked, as objective two needs to find common links before objective three can be achieved. The second objective was to identify key differences in bone due to obesity in LM, GMSA and CSSA and the third was to compare and contrast the results of LM, GMSA and CSSA. When linear measurements were compared between the three groups, the factors that presented statistically significant differences coincided with the most powerful discriminating factors found in the discriminating factor analysis (DFA). The main factor was maximum length, which is a very simple and quick measurement to be taken in the field. Our study found that the obese group had significantly longer and thinner femoral bones. This difference in bone

length could only occur before the epiphysis fuse to the femur, indicating that obesity had a significant impact on rat bone development during growth. This was also observed by Papadimitriou et al. (2006), who observed that early onset obesity in humans (defined as the onset of obesity at < 3 years of age) leads to growth acceleration. Therefore, this growth acceleration can be used as a predictor for future obesity.

Ralt (2006) also discussed the issue of obesity during childhood and found a link between low muscle mass and high fat mass (called “thrift”) which is much more commonly found in tall-obese children and reinforces the idea of obesity in childhood causing bone length and fat mass to increase at the detriment of muscle mass. The epiphysis circumference was the second most powerful discriminating factor. The control group had a larger epiphyseal diameter than the obese group, which interestingly is the opposite of what would be expected when considering the principle that epiphyses will reflect body mass most accurately (Ruff, 1987; Auerbach and Ruff, 2004). Therefore, this may be a result of inactivity on the femur, and as the obese group’s body mass increased, the activity (limited as it was) decreased further. This may have cause the bone to remodel in unused areas, perhaps also around the joints. Several studies from the field of biomechanics have found this to be the result of limited activity (Unthoff and Jaworski, 1978; Berg, et al., 2007; Sherk, et al., 2008) but contradicts the anthropological literature and should be explored further.

Geometric morphometric shape analysis identified a shortening and widening of the epiphysis alongside a thinning of the femoral neck in the obese group described through two principal components. PC1 displayed shape changes at the distal epiphysis, showing that the obese and calorie restricted groups had a shorter but broader epiphysis and explained 41% of change in the analysis. This change may allow for a higher resistance to compression forces in the knee joint. It is interesting that this change occurred in a non-active sample, indicating that it may not be solely caused by bio-mechanical stimuli. The idea of obesity-led changes to the knee joint is also discussed in a review by Sowers and Karvonen-Gutierrez (2010); however, there are no definitive studies yet to confirm or deny both our finding and that of Karvonen-Gutierrez (2010). There were also changes at the femoral neck, with the obese group having a thinner femoral neck than the control

group. Zernicke et al. (1995) also found that the femoral neck thinned in a high fat environment compared to a control diet supporting the results from our study.

PC2 only accounted for 11% of overall variance and explained some of the shape change differences between obese and calorie restricted rats; however, there was some overlap. The shape change for PC2 occurred on the most lateral point of the third trochanter and its relative height in position to the mid-section. The obese group tended to have the most lateral point at a higher location relative to the bone length than that of the calorie restricted group. This change is most likely due to muscle attachments and the changes that occur to these attachment sites in relation to fat content as the third trochanter is the largest muscle attachment site on the rat femur. The third trochanter is a fibrous enthesis which is characterised by dense fibrous connective tissue at the tendon-bone interface and cover a large surface area. The tendinous tissue of the muscle will attach to the periosteum which will exert tension. In some cases, the fibrocartilage will cause osteogenesis in the muscle attachment and bone matrix will be deposited there. The process of osteoblast activity and osteogenesis in enthesal areas is still poorly understood and warrants further investigation to better apprehend the changes in enthesal development position in obese rats. Alternatively, the higher position of the third trochanter could be the result of the differences in bone length as the obese group had significantly longer maximum length measurements compared to the control group. Should diaphyseal modelling occur mainly in the diaphysis distal to the third trochanter than its relatively higher position would merely be a by-product of length increase.

Rabey et al. (2015) indicated that muscle size and strength does not affect muscle attachment sites and although this contradicts the anthropological literature (e.g. Vilotte, 2013), this would allow the activity factor (or lack of) to be removed from the discussion and therefore support the longitudinal growth as cause for the position of the third trochanter. It is worth noting that throughout all the principle components, the femoral head and the mid-shaft area were not significantly different between the three groups and suggests that the effects of obesity are isolated and do not interfere with the mechanics of the proximal femur.

For the midshaft CSSA the two factors that were most discriminatory in both canonical functions were IY (i.e., bending rigidity in the medio-lateral direction) and ZY (bending

strength in the medio-lateral direction). At the third trochanter, the two most influential factors were IY and IX (bending rigidity in the medio-lateral and antero-posterior directions respectively). The second canonical function showed changes in Zp (overall strength of bone) and MaxRad (the maximum radial dimension distance).

All the tests several results in common, with each supporting the claims of the other. For example, the changes in bone length identified by the linear measurements are reinforced by the relative location change of the third trochanter by GMSA. The reduction in midshaft circumference found by linear measurements is also reinforced by the biomechanical analysis of the midshaft. The CSSA found that bending rigidity in the obese sample was increased, which would be expected from a thinner bone.

The fourth objective was to determine whether bone changes due to obesity are permanent or reversible by studying the calorie restricted group. Several tests showed no significant differences between RE and CC, and yet others could distinguish between all three groups in most cases. An example of a test that could not distinguish between RE and CC was the biomechanical analysis of the midshaft and trochanter. This means that within a relatively short period, the internal dimensions of bone had reversed to their original state. However, an interesting contradiction of results can be found in GMSA, as this defined a clear external shape change between CC and RE as PC1 (41% of shape difference) did not separate CO and RE but clearly separated CC. Both results suggest that the internal structures of bone remodel far faster than the externals. To further understand the long-term effects of weight loss on bone structure and remodelling, a further experiment would be required that continues for a longer period before sacrifice. This would then be able to compare to the current findings and assess the changes over time in much further detail.

The aims of this study were very broad and exploratory to an extent. Nevertheless, the aims were reached. The first aim was to form initial insights into how obesity affects bone health during development using methodologies and techniques from several fields of science. There were two separate fields of science used during this study; biological anthropology and biomechanics. Both linear measurements and geometric morphometric shape analysis are techniques used in biological anthropology, with cross-sectional shape analysis being used in biomechanics. The three techniques complement each other due to

the core similarities of measuring dimensions of bone, albeit in different ways. By analysing several different dimensions of bone at the same time, a clearer image of overall changes can be identified, each backed up by different analysis.

The second aim was to understand how different scientific fields can be used to answer complex questions. For example, if GMSA was performed by itself on the data set, the finding of RE not remodelling at a uniform rate throughout bone would not have been found, furthering our understanding of morphological processes. Also, different fields may already have a method/technique of identifying and measuring an outcome that currently cannot be measured in a specified field.

The third aim was to further understand the effect of obesity on bone as a tool to identifying obesity in ancient populations. Therefore, understanding how obesity affected society throughout human history and civilisation. This still requires more work, although this study gives hints of interesting signs in this preliminary study. For example, a femur that has a flat broad distal epiphysis but also a long thin diaphysis is more likely to have belonged to an obese individual than an individual of normal weight. This aspect requires further sample analysis of known populations which may lead to a way of identifying obese individuals in past human populations.

The fourth aim was to identify how obesity affects bone during developmental periods as an aid for understanding modern day societal pressures of obesity. Using the fourth objective of determining changes in the RE group in comparison to both the CC and CO group we can start unpicking the changes to bone due to weight loss. The key findings of this study are that changes to bone due to obesity during development are reversible, but to what extent is still unknown due to the sample used in this study. As previously mentioned, a further experimental study would need to be conducted to fully identify the full remodelling process due to weight loss.

Conclusion

The use of methods from the field of anthropology, a discipline specialised in the study of bone, allowed us to use an experimental set-up to determine and isolate the effects of obesity on bone health. This study has revealed novel insights into the effects of gravitational forces on body mass due to obesity without the influence of muscle forces on the bone. This was facilitated using metabolic cages where movement was restricted due to the minimal space in the cage. This experimental set-up allowed us to say with much more certainty that any changes in external and internal shape are due to the dietary conditions of the rats and not due to differences in activity levels.

When all the results are considered together it paints an interesting picture. All tests distinguished between obesity and control with relative ease but the calorie restricted group was more variable. Obese individuals had longer femora with a relatively higher positioned third trochanter but were more gracile and weaker in their diaphyseal strength and rigidity compared to the control sample. These findings confirm that obesity has a significant effect on bone shape and strength.

The calorie restricted group was almost identical to the obese group in external overall bone shape, with only minor shape variation (11%) in the position of the most lateral point of the third trochanter. In comparison, internal cross-sectional shape analysis suggests that the calorie restricted group were more closely related to the control group, especially at the third trochanter where there was clear separation from the obese group. These results support our third hypothesis that a period of calorie restriction for obese rats will reduce the effect of obesity on bone shape and strength. Calorie restriction does not affect all bone properties simultaneously. The bone will re-model after weight loss but the internal structures need to re-arrange before the external structures can do so. The process of this needs to be further investigated.

Overall, this study has provided a new approach to the study of obesity and its effect on bone morphology – a topic poorly investigated in the field of study of ancient human skeletons and physiology alike. By using methods developed within the field of anthropology and applying it in an experimental approach we have been able to bear new information of the influence of diet and obesity on bone morphology which will be of use

for the study of past human populations. We were also able to shed light on the effect of obesity as a current societal challenge on bone health.

Future directions

The original sample provided to us by the partners contained 54 rats in 6 different groups (n=9rats/group). The groups not yet discussed were as follows: HFDJ: High-Fat high-sucrose Diet-induced obesity Juveniles; RES: diet-induced obesity supplemented with Resveratrol; and R+R: diet-induced obesity subjected to caloric Restriction and supplemented with Resveratrol. These groups would benefit from future research in addition to this study due to the wide range of questions that these additional groups might answer. For example, what are the effects of a high fat diet during growth periods?

The relationship between length, muscle mass and fat mass need to be further investigated. For example, the juvenile group (HFDJ) that is available could be compared to a control group sacrificed at the same age. The samples could be injected with dyes, designed to target and bind to the three different bone cell types; osteoblasts, osteoclasts and osteocytes. This would enable researchers to identify areas of bone growth and loss in the bones of the young rodents and determine if fat content is affecting the formation of bones in adolescence and how the processes of modelling (growth and length increase) and remodelling (loss in bone mass and strength) are interacting.

Other future directions of this work would be to look at the cellular biology, elemental composition and density of the bone samples. Cellular biology can be studied using immunohistochemistry, Western blot and general staining with light microscopy. Immunohistochemistry targets specific proteins with an antibody attached to a fluorochrome which can be seen under different conditions, allowing quantification. One way of doing so is by targeting the protein called osteocalcin, which is highly linked to osteoblasts, the bone forming cells, and is thought to also regulate insulin release from the pancreas and leptin from adipocytes (Lee et al., 2007). Both factors are of interest with osteocalcin, as the distribution of osteocalcin will show the areas of bone formation and the overall quantity will reveal the effect this will have on insulin and leptin levels, both key factors in diabetes.

Elemental composition of bone could be analysed by using scanning electron microscopy and energy dispersive microscopy (SEM/EDAX). This technique uses the atomic signature detected by X-ray absorption in the sample as each element has unique absorption values depending on its energy level. Not only does SEM/EDAX detect which elements are present but it also allows for quantification. This allows for a full elemental composition of each sample and thus for comparison between groups. The main elements of interest with regards to bone are potassium, iron and calcium. Changes in these elemental distributions between the three groups may determine how different diets can affect the uptake or storage of different trace elements. A similar technique is used for biomonitoring of trace elements from atmospheric pollution (Tomašević and Aničić, 2010).

Density analysis could be performed using the microCT scans in Avizo 9, as described for the present study, and could further explore the physical composition of bone. To this end, density phantoms were included in the scans which can be used to obtain relative density for each sample. Bone density is of special interest due to its high correlation with osteoporosis, especially in older individuals, and is measured through bone mineral density analysis (Kanis, 2002).

The completion of all the analyses mentioned above would significantly increase our understanding of how obesity affects bone, both structurally and at the cellular level.

References

- Aarden, E.M., Nijweide, P.J. and Burger, E.H., 1994. Function of osteocytes in bone. *Journal of Cellular Biochemistry*, 55(3), pp.287-299.
- Adams, D.C., Rohlf, F.J. and Slice, D.E., 2004. Geometric morphometrics: ten years of progress following the 'revolution'. *Italian Journal of Zoology*, 71(1), pp.5-16.
- Atkins, G.J. and Findlay, D.M., 2012. Osteocyte regulation of bone mineral: a little give and take. *Osteoporosis International*, 23(8), pp.2067-2079.
- Atkins, G.J., Rowe, P.S., Lim, H.P., Welldon, K.J., Ormsby, R., Wijenayaka, A.R., Zelenchuk, L., Evdokiou, A. and Findlay, D.M., 2011. Sclerostin is a locally acting regulator of late-osteoblast/preosteocyte differentiation and regulates mineralization through a MEPE-ASARM-dependent mechanism. *Journal of Bone and Mineral Research*, 26(7), pp.1425-1436.
- Atterton, T., De Groote, I. and Eliopoulos, C., 2016. Assessing size and strength of the clavicle for its usefulness for sex estimation in a British medieval sample. *HOMO-Journal of Comparative Human Biology*, 67(5), pp.409-416.
- Auerbach, B.M. and Ruff, C.B., 2004. Human body mass estimation: a comparison of "morphometric" and "mechanical" methods. *American Journal of Physical Anthropology*, 125(4), pp.331-342.
- Beck, T.J., Petit, M.A., Wu, G., LeBoff, M.S., Cauley, J.A. and Chen, Z., 2009. Does Obesity Really Make the Femur Stronger? BMD, Geometry, and Fracture Incidence in the Women's Health Initiative-Observational Study. *Journal of Bone and Mineral Research*, 24(8), pp.1369-1379.
- Beresford, J.N., Bennett, J.H., Devlin, C., Leboy, P.S. and Owen, M.E., 1992. Evidence for an inverse relationship between the differentiation of adipocytic and osteogenic cells in rat marrow stromal cell cultures. *Journal of Cell Science*, 102(2), pp.341-351.
- Berg, H.E., Eiken, O., Miklavcic, L. and Mekjavic, I.B., 2007. Hip, thigh and calf muscle atrophy and bone loss after 5-week bedrest inactivity. *European Journal of Applied Physiology*, 99(3), pp.283-289.

- Bonewald, L.F. and Johnson, M.L., 2008. Osteocytes, mechanosensing and Wnt signaling. *Bone*, 42(4), pp.606-615.
- Bose, K., Bhadra, M. and Mukhopadhyay, A., 2007. Causes and consequences of obesity. *Anthropology Today: Trends, Scope and Applications*, pp.223-240.
- Boskey, A.L., 1996. Matrix proteins and mineralization: an overview. *Connective Tissue Research*, 35(1-4), pp.357-363.
- Boskey, A.L., 1998. Biomineralization: conflicts, challenges, and opportunities. *Journal of Cellular Biochemistry*, 72(S30-31), pp.83-91.
- Bossard, M.J., Tomaszek, T.A., Thompson, S.K., Amegadzie, B.Y., Hanning, C.R., Jones, C., Kurdyla, J.T., McNulty, D.E., Drake, F.H., Gowen, M. and Levy, M.A., 1996. Proteolytic activity of human osteoclast cathepsin K expression, purification, activation, and substrate identification. *Journal of Biological Chemistry*, 271(21), pp.12517-12524.
- Boulet, L.P., 2013. Asthma and obesity. *Clinical & Experimental Allergy*, 43(1), pp.8-21.
- Brown, C.D., Higgins, M., Donato, K.A., Rohde, F.C., Garrison, R., Obarzanek, E., Ernst, N.D. and Horan, M., 2000. Body mass index and the prevalence of hypertension and dyslipidemia. *Obesity Research*, 8(9), pp.605-619.
- Bouxsein, M.L., 2003. Bone quality: an old concept revisited. *Osteoporosis International*, 14(05), pp.1-2.
- Burr, D.B., Forwood, M.R., Fyhrie, D.P., Martin, R.B., Schaffler, M.B. and Turner, C.H., 1997. Bone microdamage and skeletal fragility in osteoporotic and stress fractures. *Journal of Bone and Mineral Research*, 12(1), pp.6-15.
- Cao, J.J., Gregoire, B.R. and Gao, H., 2009. High-fat diet decreases cancellous bone mass but has no effect on cortical bone mass in the tibia in mice. *Bone*, 44(6), pp.1097-1104.
- Cawley, J. and Meyerhoefer, C., 2012. The medical care costs of obesity: an instrumental variables approach. *Journal of Health Economics*, 31(1), pp.219-230.
- Chandra, R.K., 1981. Immunodeficiency in undernutrition and overnutrition. *Nutrition Reviews*, 39(6), pp.225-231.

- Cicutтини, F.M., Baker, J.R. and Spector, T.D., 1996. The association of obesity with osteoarthritis of the hand and knee in women: a twin study. *J Rheumatol*, 23(7), pp.1221-1226.
- Cirmanova, V., Bayer, M., Starka, L. and Zajickova, K., 2008. The effect of leptin on bone—an evolving concept of action. *Physiological Research*, 57, pp.143-151.
- Dallas, S.L., Prideaux, M. and Bonewald, L.F., 2013. The osteocyte: an endocrine cell... and more. *Endocrine Reviews*, 34(5), pp.658-690.
- De Laet, C., Kanis, J.A., Odén, A., Johanson, H., Johnell, O., Delmas, P., Eisman, J.A., Kroger, H., Fujiwara, S., Garnero, P. and McCloskey, E.V., 2005. Body mass index as a predictor of fracture risk: a meta-analysis. *Osteoporosis International*, 16(11), pp.1330-1338.
- Denke, M.A., Sempos, C.T. and Grundy, S.M., 1994. Excess body weight: an under-recognized contributor to dyslipidemia in white American women. *Archives of Internal Medicine*, 154(4), pp.401-410.
- Deurenberg, P. and Yap, M., 1999. The assessment of obesity: methods for measuring body fat and global prevalence of obesity. *Best Practice & Research Clinical Endocrinology & Metabolism*, 13(1), pp.1-11.
- Dorheim, M.A., Sullivan, M., Dandapani, V., Wu, X., Hudson, J., Segarini, P.R., Rosen, D.M., Aulthouse, A.L. and Gimble, J.M., 1993. Osteoblastic gene expression during adipogenesis in hematopoietic supporting murine bone marrow stromal cells. *Journal of Cellular Physiology*, 154(2), pp.317-328.
- Ducy, P., Desbois, C., Boyce, B., Pinero, G., Story, B., Dunstan, C., Smith, E., Bonadio, J., Goldstein, S., Gundberg, C. and Bradley, A., 1996. Increased bone formation in osteocalcin-deficient mice. *Nature*, 382(6590), pp.448-452.
- Durnin, J.V. and Womersley, J.V.G.A., 1974. Body fat assessed from total body density and its estimation from skinfold thickness: measurements on 481 men and women aged from 16 to 72 years. *British journal of nutrition*, 32(01), pp.77-97.

- Eckel, R.H., Kahn, R., Robertson, R.M. and Rizza, R.A., 2006. Preventing cardiovascular disease and diabetes A call to action from the American Diabetes Association and the American Heart Association. *Circulation*, 113(25), pp.2943-2946.
- Ellis, K.J., Shypailo, R.J., Wong, W.W. and Abrams, S.A., 2003. Bone mineral mass in overweight and obese children: diminished or enhanced? *Acta Diabetologica*, 40(1), pp.274-277.
- Felsenberg, D. and Boonen, S., 2005. The bone quality framework: determinants of bone strength and their interrelationships, and implications for osteoporosis management. *Clinical Therapeutics*, 27(1), pp.1-11.
- Felson, D.T., Zhang, Y., Hannan, M.T. and Anderson, J.J., 1993. Effects of weight and body mass index on bone mineral density in men and women: the Framingham study. *Journal of Bone and Mineral Research*, 8(5), pp.567-573.
- Gimble, J.M., Robinson, C.E., Wu, X. and Kelly, K.A., 1996. The function of adipocytes in the bone marrow stroma: an update. *Bone*, 19(5), pp.421-428.
- Guillaume, M., 1999. Defining obesity in childhood: current practice. *The American Journal of Clinical Nutrition*, 70(1), pp.126S-130S.
- Hajjawi, M.O., MacRae, V.E., Huesa, C., Boyde, A., Millán, J.L., Arnett, T.R. and Orriss, I.R., 2014. Mineralisation of collagen rich soft tissues and osteocyte lacunae in *Enpp1*^{-/-} mice. *Bone*, 69, pp.139-147.
- Hamrick, M.W. and Ferrari, S.L., 2008. Leptin and the sympathetic connection of fat to bone. *Osteoporosis International*, 19(7), pp.905-912.
- Hart, D.J. and Spector, T.D., 1993. The relationship of obesity, fat distribution and osteoarthritis in women in the general population: the Chingford Study. *The Journal of Rheumatology*, 20(2), pp.331-335.
- Hawkey, D.E. and Street, S., 1992. Activity-induced stress markers in prehistoric human remains from the eastern Aleutian Islands. *American Journal of Physical Anthropology*, 14, pp.89-89.

- Hayashida, C., Ito, J., Nakayachi, M., Okayasu, M., Ohyama, Y., Hakeda, Y. and Sato, T., 2014. Osteocytes produce interferon- β as a negative regulator of osteoclastogenesis. *Journal of Biological Chemistry*, 289(16), pp.11545-11555.
- Hayman, A.R., Jones, S.J., Boyde, A., Foster, D., Colledge, W.H., Carlton, M.B., Evans, M.J. and Cox, T.M., 1996. Mice lacking tartrate-resistant acid phosphatase (Acp 5) have disrupted endochondral ossification and mild osteopetrosis. *Development*, 122(10), pp.3151-3162.
- Honma, M., Ikebuchi, Y., Kariya, Y., Hayashi, M., Hayashi, N., Aoki, S. and Suzuki, H., 2013. RANKL subcellular trafficking and regulatory mechanisms in osteocytes. *Journal of Bone and Mineral Research*, 28(9), pp.1936-1949.
- Horlick, M., Wang, J., Pierson, R.N. and Thornton, J.C., 2004. Prediction models for evaluation of total-body bone mass with dual-energy X-ray absorptiometry among children and adolescents. *Pediatrics*, 114(3), pp. 337-345.
- Javaheri, B., Carriero, A., Staines, K.A., Chang, Y.M., Houston, D.A., Oldknow, K.J., Millan, J.L., Kazeruni, B.N., Salmon, P., Shefelbine, S. and Farquharson, C., 2015. Phospho1 deficiency transiently modifies bone architecture yet produces consistent modification in osteocyte differentiation and vascular porosity with ageing. *Bone*, 81, pp.277-291.
- Jebb, S.A. and Elia, M., 1993. Techniques for the measurement of body composition: a practical guide. *International Journal of Obesity and Related Metabolic Disorders: Journal of the International Association for the Study of Obesity*, 17(11), pp.611-621.
- Jee, W.S. and Li, X.J., 1990. Adaptation of cancellous bone to overloading in the adult rat: a single photon absorptiometry and histomorphometry study. *The anatomical record*, 227(4), pp.418-426.
- Jiang, J.X., Siller-Jackson, A.J. and Burra, S., 2007. Roles of gap junctions and hemichannels in bone cell functions and in signal transmission of mechanical stress. *Frontiers in Bioscience: A Journal and Virtual Library*, 12, p.1450.
- Johns Hopkins School of Medicine. Calculating Moments 2015 [updated 1 July 2015; cited 2015 3 September]. Available from: <http://www.hopkinsmedicine.org/fae/mmacro.html>.
- Jolliffe, I., 2002. Principal component analysis. John Wiley & Sons, Ltd.

- Józsa, L.G., 2011. Obesity in the paleolithic era. *Hormones*, 10(3), pp.241-244.
- Jurmain, R. and Villotte, S., 2010. Terminology. Entheses in medical literature and physical anthropology: a brief review. In Document published online in 4th February following the Workshop in Musculoskeletal Stress Markers (MSM): Limitations and Achievements in the Reconstruction of Past Activity Patterns (pp. 2-3).
- Jurmain, R., Cardoso, F.A., Henderson, C. and Villotte, S., 2012. Bioarchaeology's Holy Grail: the reconstruction of activity. *A Companion to Paleopathology*, pp.531-552.
- Kanders, B.S., Lavin, P.T., Kowalchuk, M.B., Greenberg, I. and Blackburn, G.L., 1988. An evaluation of the effect of aspartame on weight loss. *Appetite*, 11, pp.73-84.
- Kanis, J.A., Borgstrom, F., De Laet, C., Johansson, H., Johnell, O., Jonsson, B., Oden, A., Zethraeus, N., Pfeleger, B. and Khaltsev, N., 2005. Assessment of fracture risk. *Osteoporosis International*, 16(6), pp.581-589.
- Kanis, J.A., 2002. Diagnosis of osteoporosis and assessment of fracture risk. *The Lancet*, 359(9321), pp.1929-1936.
- Kelley, J.O. and Angel, J.L., 1987. Life stresses of slavery. *American Journal of Physical Anthropology*, 74(2), pp.199-211.
- Kenchiah, S., Evans, J.C., Levy, D., Wilson, P.W., Benjamin, E.J., Larson, M.G., Kannel, W.B. and Vasan, R.S., 2002. Obesity and the risk of heart failure. *New England Journal of Medicine*, 347(5), pp.305-313.
- Kennedy, K.A., 1989. Skeletal markers of occupational stress. *Reconstruction of Life from the Skeleton*, pp.129-160.
- Khosla, S., Riggs, B.L., Atkinson, E.J., Oberg, A.L., McDaniel, L.J., Holets, M., Peterson, J.M. and Melton, L.J., 2006. Effects of sex and age on bone microstructure at the ultradistal radius: a population-based noninvasive in vivo assessment. *Journal of Bone and Mineral Research*, 21(1), pp.124-131.
- Kogawa, M., Wijenayaka, A.R., Ormsby, R.T., Thomas, G.P., Anderson, P.H., Bonewald, L.F., Findlay, D.M. and Atkins, G.J., 2013. Sclerostin regulates release of bone mineral by osteocytes by induction of carbonic anhydrase 2. *Journal of Bone and Mineral Research*, 28(12), pp.2436-2448.

- Lac, G., Cavalie, H., Ebal, E. and Michaux, O., 2008. Effects of a high fat diet on bone of growing rats. Correlations between visceral fat, adiponectin and bone mass density. *Lipids in Health and Disease*, 7(1), pp.1-4
- Lecka-Czernik, B., Gubrij, I., Moerman, E.J., Kajkenova, O., Lipschitz, D.A., Manolagas, S.C. and Jilka, R.L., 1999. Inhibition of *Osf2/Cbfa1* expression and terminal osteoblast differentiation by PPAR γ 2. *Journal of Cellular Biochemistry*, 74(3), pp.357-371.
- Lee, N.K., Sowa, H., Hinoi, E., Ferron, M., Ahn, J.D., Confavreux, C., Dacquin, R., Mee, P.J., McKee, M.D., Jung, D.Y. and Zhang, Z., 2007. Endocrine regulation of energy metabolism by the skeleton. *Cell*, 130(3), pp.456-469.
- Lee, S.S. and Piazza, S.J., 2009. Built for speed: musculoskeletal structure and sprinting ability. *Journal of Experimental Biology*, 212(22), pp.3700-3707.
- Lieberman, D.E., Polk, J.D. and Demes, B., 2004. Predicting long bone loading from cross-sectional geometry. *American Journal of Physical Anthropology*, 123(2), pp.156-171.
- Lloyd, J.K. and Wolff, O.H., 1980. Overnutrition and obesity. *Prevention in Childhood of Health Problems in Adult Life*, pp.53-70.
- Madsen, K.L., Adams, W.C. and Van Loan, M.D., 1998. Effects of physical activity, body weight and composition, and muscular strength on bone density in young women. *Medicine and science in sports and exercise*, 30(1), pp.114-120.
- Manolagas, S.C., 2000. Birth and death of bone cells: basic regulatory mechanisms and implications for the pathogenesis and treatment of osteoporosis 1. *Endocrine reviews*, 21(2), pp.115-137.
- Melton, L.J., Leibson, C.L., Achenbach, S.J., Therneau, T.M. and Khosla, S., 2008. Fracture risk in type 2 diabetes: update of a population-based study. *Journal of Bone and Mineral Research*, 23(8), pp.1334-1342.
- Merbs, C.F., 1983. Patterns of activity-induced pathology in a Canadian Inuit population. *Musée National de l'Homme. Collection Mercure. Commission Archéologique du Canada. Publications d'Archéologie. Dossier Ottawa*, (119), pp.1-199.

Mokdad, A.H., Ford, E.S., Bowman, B.A., Dietz, W.H., Vinicor, F., Bales, V.S. and Marks, J.S., 2003. Prevalence of obesity, diabetes, and obesity-related health risk factors, 2001. *Jama*, 289(1), pp.76-79.

Must, A., Spadano, J., Coakley, E.H., Field, A.E., Colditz, G. and Dietz, W.H., 1999. The disease burden associated with overweight and obesity. *Jama*, 282(16), pp.1523-1529.

Nakashima, T., Hayashi, M., Fukunaga, T., Kurata, K., Oh-hora, M., Feng, J.Q., Bonewald, L.F., Kodama, T., Wutz, A., Wagner, E.F. and Penninger, J.M., 2011. Evidence for osteocyte regulation of bone homeostasis through RANKL expression. *Nature Medicine*, 17(10), pp.1231-1234.

Nesbitt, S.A. and Horton, M.A., 1997. Trafficking of matrix collagens through bone-resorbing osteoclasts. *Science*, 276(5310), pp.266-269.

Ng, M., Fleming, T., Robinson, M., Thomson, B., Graetz, N., Margono, C., Mullany, E.C., Biryukov, S., Abbafati, C., Abera, S.F. and Abraham, J.P., 2014. Global, regional, and national prevalence of overweight and obesity in children and adults during 1980–2013: a systematic analysis for the Global Burden of Disease Study 2013. *The Lancet*, 384(9945), pp.766-781.

Nijweide PJ, Burger EH, Klein-Nulend J, van der Pluijm G., 1996. The Osteocyte. In: Bilezikian JP, Raisz LG, Rodan GA (eds) *Principles of Bone Biology*. Academic Press, San Diego, CA, pp 115–126

Ogden, C.L., Carroll, M.D., Kit, B.K. and Flegal, K.M., 2014. Prevalence of childhood and adult obesity in the United States, 2011-2012. *Jama*, 311(8), pp.806-814.

Palumbo, C., Palazzini, S. and Marotti, G., 1990. Morphological study of intercellular junctions during osteocyte differentiation. *Bone*, 11(6), pp.401-406.

Papadimitriou, A., Gousi, T., Giannouli, O. and Nicolaidou, P., 2006. The growth of children in relation to the timing of obesity development. *Obesity*, 14(12), pp.2173-2176.

Parfitt, A.M., 1994. Osteonal and hemi-osteonal remodeling: the spatial and temporal framework for signal traffic in adult human bone. *Journal of Cellular Biochemistry*, 55(3), pp.273-286.

- Patsch, J.M., Kiefer, F.W., Varga, P., Pail, P., Rauner, M., Stupphann, D., Resch, H., Moser, D., Zysset, P.K., Stulnig, T.M. and Pietschmann, P., 2011. Increased bone resorption and impaired bone microarchitecture in short-term and extended high-fat diet-induced obesity. *Metabolism*, 60(2), pp.243-249.
- Pietrobelli, A., et al., 1996. Dual-energy X-ray absorptiometry body composition model: review of physical concepts. *American Journal of Physiology-Endocrinology And Metabolism*, 271(6), pp.E941-E951
- Pocock, N., Eisman, J., Gwinn, T., Sambrook, P., Kelly, P., Freund, J. and Yeates, M., 1989. Muscle strength, physical fitness, and weight but not age predict femoral neck bone mass. *Journal of Bone and Mineral Research*, 4(3), pp.441-448.
- Prentice, A., Parsons, T.J. and Cole, T.J., 1994. Uncritical use of bone mineral density in absorptiometry may lead to size-related artifacts in the identification of bone mineral determinants. *The American Journal of Clinical Nutrition*, 60(6), pp.837-842.
- Prideaux, M., Findlay, D.M. and Atkins, G.J., 2016. Osteocytes: the master cells in bone remodelling. *Current Opinion in Pharmacology*, 28, pp.24-30.
- Qing, H., Ardeshirpour, L., Divieti Pajevic, P., Dusevich, V., Jähn, K., Kato, S., Wysolmerski, J. and Bonewald, L.F., 2012. Demonstration of osteocytic perilacunar/canalicular remodeling in mice during lactation. *Journal of Bone and Mineral Research*, 27(5), pp.1018-1029.
- Rabey, K.N., Green, D.J., Taylor, A.B., Begun, D.R., Richmond, B.G. and McFarlin, S.C., 2015. Locomotor activity influences muscle architecture and bone growth but not muscle attachment site morphology. *Journal of Human Evolution*, 78, pp.91-102.
- Ralt, D., 2006. The muscle-fat duel or why obese children are taller? *BMC Pediatrics*, 6(1), pp.1-4
- Rho, J.Y., Kuhn-Spearing, L. and Zioupos, P., 1998. Mechanical properties and the hierarchical structure of bone. *Medical Engineering & Physics*, 20(2), pp.92-102.
- Robey PG, Boskey AL 1995 The biochemistry of bone. In: Marcus R, Feldman D, Bilezikian JP, Kelsey J (eds) *Osteoporosis*. Academic Press, New York, pp.95-183

- Roodman, G.D., 1996. Advances in Bone Biology: The Osteoclast*. *Endocrine Reviews*, 17(4), pp.308-332.
- Roodman, G.D., Hughes, D.E. and Boyce, B.F., 1996. A new model for the regulation of bone resorption, with particular reference to the effects of biphosphonates. *J Bone Miner Res*, 11(2), pp.150-159
- Rosen, C.J. and Bouxsein, M.L., 2006. Mechanisms of disease: is osteoporosis the obesity of bone?. *Nature clinical practice Rheumatology*, 2(1), pp.35-43.
- Ruff, C., 1987. Sexual dimorphism in human lower limb bone structure: relationship to subsistence strategy and sexual division of labor. *Journal of Human Evolution*, 16(5), pp.391-416.
- Ruff, C.B., 1991. Climate and body shape in hominid evolution. *Journal of Human Evolution*, 21(2), pp.81-105.
- Ruff, C., 2008. Femoral/humeral strength in early African Homo erectus. *Journal of Human Evolution*, 54(3), pp.383-390.
- Salo, J., Lehenkari, P., Mulari, M., Metsikkö, K. and Väänänen, H.K., 1997. Removal of osteoclast bone resorption products by transcytosis. *Science*, 276(5310), pp.270-273.
- Sarringhaus, L.A., Stock, J.T., Marchant, L.F. and McGrew, W.C., 2005. Bilateral asymmetry in the limb bones of the chimpanzee (*Pan troglodytes*). *American Journal of Physical Anthropology*, 128(4), pp.840-845.
- Shaw, C.N. and Stock, J.T., 2009. Habitual throwing and swimming correspond with upper limb diaphyseal strength and shape in modern human athletes. *American Journal of Physical Anthropology*, 140(1), pp.160-172.
- Sherk, V.D., Bembien, M.G. and Bembien, D.A., 2008. BMD and bone geometry in transtibial and transfemoral amputees. *Journal of Bone and Mineral Research*, 23(9), pp.1449-1457.
- Slemenda, C.W., Hui, S.L., Longcope, C., Wellman, H. and Johnston, C.C., 1990. Predictors of bone mass in perimenopausal women: a prospective study of clinical data using photon absorptiometry. *Annals of Internal Medicine*, 112(2), pp.96-101.

- Sowers, M.R. and Karvonen-Gutierrez, C.A., 2010. The evolving role of obesity in knee osteoarthritis. *Current Opinion in Rheumatology*, 22(5), p.533
- Steppan, C.M., Bailey, S.T., Bhat, S., Brown, E.J., Banerjee, R.R., Wright, C.M., Patel, H.R., Ahima, R.S. and Lazar, M.A., 2001. The hormone resistin links obesity to diabetes. *Nature*, 409(6818), pp.307-312.
- Stock, J.T. and Pfeiffer, S.K., 2004. Long bone robusticity and subsistence behaviour among Later Stone Age foragers of the forest and fynbos biomes of South Africa. *Journal of Archaeological Science*, 31(7), pp.999-1013.
- Stock, J.T. and Shaw, C.N., 2007. Which measures of diaphyseal robusticity are robust? A comparison of external methods of quantifying the strength of long bone diaphyses to cross-sectional geometric properties. *American Journal of Physical Anthropology*, 134(3), pp.412-423.
- Stock, J.T., 2002. A test of two methods of radiographically deriving long bone cross-sectional properties compared to direct sectioning of the diaphysis. *International Journal of Osteoarchaeology*, 12(5), pp.335-342.
- Tang, S.Y., Herber, R.P., Ho, S.P. and Alliston, T., 2012. Matrix metalloproteinase-13 is required for osteocytic perilacunar remodeling and maintains bone fracture resistance. *Journal of Bone and Mineral Research*, 27(9), pp.1936-1950.
- Thomas, T. and Burguera, B., 2002. Is leptin the link between fat and bone mass? *Journal of Bone and Mineral Research*, 17(9), pp.1563-1569.
- Tomašević, M. and Aničić, M., 2010. Trace element content in urban tree leaves and SEM-EDAX characterization of deposited particles. *Facta Universitatis-Series: Physics, Chemistry and Technology*, 8(1), pp.1-13.
- Tomkinson, A., Gevers, E.F., Wit, J.M., Reeve, J. and Noble, B.S., 1998. The role of estrogen in the control of rat osteocyte apoptosis. *Journal of Bone and Mineral Research*, 13(8), pp.1243-1250.
- Tomkinson, A., Reeve, J., Shaw, R.W. and Noble, B.S., 1997. The Death of Osteocytes via Apoptosis Accompanies Estrogen Withdrawal in Human Bone 1. *The Journal of Clinical Endocrinology & Metabolism*, 82(9), pp.3128-3135.

- Udagawa, N., Takahashi, N., Akatsu, T., Tanaka, H., Sasaki, T., Nishihara, T., Koga, T., Martin, T.J. and Suda, T., 1990. Origin of osteoclasts: mature monocytes and macrophages are capable of differentiating into osteoclasts under a suitable microenvironment prepared by bone marrow-derived stromal cells. *Proceedings of the National Academy of Sciences*, 87(18), pp.7260-7264.
- Uthoff, H.K. and Jaworski, Z.F., 1978. Bone loss in response to long-term immobilisation. *Bone & Joint Journal*, 60(3), pp.420-429.
- Van Gaal, L.F., Mertens, I.L. and Christophe, E., 2006. Mechanisms linking obesity with cardiovascular disease. *Nature*, 444(7121), pp.875-880.
- Villotte, S. and Knüsel, C.J., 2013. Understanding enthesal changes: definition and life course changes. *International Journal of Osteoarchaeology*, 23(2), pp.135-146.
- Villotte, S., Castex, D., Couallier, V., Dutour, O., Knüsel, C.J. and Henry-Gambier, D., 2010. Enthesopathies as occupational stress markers: evidence from the upper limb. *American Journal of Physical Anthropology*, 142(2), pp.224-234.
- Weinstein, R.S., Jilka, R.L., Parfitt, A.M. and Manolagas, S.C., 1998. Inhibition of osteoblastogenesis and promotion of apoptosis of osteoblasts and osteocytes by glucocorticoids. Potential mechanisms of their deleterious effects on bone. *Journal of Clinical Investigation*, 102(2), p.274.
- Weiss, E., 2007. Muscle markers revisited: activity pattern reconstruction with controls in a central California Amerind population. *American Journal of Physical Anthropology*, 133(3), pp.931-940.
- Wijenayaka, A.R., Kogawa, M., Lim, H.P., Bonewald, L.F., Findlay, D.M. and Atkins, G.J., 2011. Sclerostin stimulates osteocyte support of osteoclast activity by a RANKL-dependent pathway. *PloS one*, 6(10), p.e25900.
- Whyte, M.P., 1994. Hypophosphatasia and the Role of Alkaline Phosphatase in Skeletal Mineralization*. *Endocrine Reviews*, 15(4), pp.439-461.
- Xiong, J., Onal, M., Jilka, R.L., Weinstein, R.S., Manolagas, S.C. and O'brien, C.A., 2011. Matrix-embedded cells control osteoclast formation. *Nature Medicine*, 17(10), pp.1235-1241.

Zernicke, R.F., Salem, G.J., Barnard, R.J. and Schramm, E., 1995. Long-term, high-fat-sucrose diet alters rat femoral neck and vertebral morphology, bone mineral content, and mechanical properties. *Bone*, 16(1), pp.25-31.

Zumwalt, A., 2006. The effect of endurance exercise on the morphology of muscle attachment sites. *Journal of Experimental Biology*, 209(3), pp.444-454.